ASSESSING THE REHABILITATION STATUS OF THE REFLOODED BAHIA GRANDE, TEXAS BASED ON TRACE GAS FLUXES, BENTHIC MACROINVERTEBRATES, AND FISH COMMUNITY DATA ALONG SALINITY AND SEAGRASS GRADIENTS

A Thesis

by

CATHERINE M. ECKERT

Submitted to the Graduate College of
The University of Texas Rio Grande Valley
In partial fulfillment of the requirements for the degree of

MASTER OF SCIENCE

December 2019

Major Subject: Biology

ASSESSING THE REHABILITATION STATUS OF THE REFLOODED BAHIA GRANDE, TEXAS BASED ON TRACE GAS FLUXES, BENTHIC MACROINVERTEBRATES, AND FISH COMMUNITY DATA ALONG SALINITY AND SEAGRASS GRADIENTS

A Thesis
by
CATHERINE M. ECKERT

COMMITTEE MEMBERS

Dr. David Hicks
Chair of Committee

Dr. Alejandro Fierro
Committee Member

Dr. Abdullah Rahman
Committee Member

December 2019

ABSTRACT

Eckert, Catherine M., Assessing the Rehabilitation Status of the Reflooded Bahia Grande, Texas Based on Trace Gas Fluxes, Benthic Macroinvertebrates, and Fish Community Data Along Salinity and Seagrass Gradients. Master of Science (MS), December, 2019, 95 pp., 8 tables, 26 figures, 79 references, 38 titles.

The Bahia Grande is a 6,500-acre tidal basin located at the southernmost tip of Texas. Tidal flow into this coastal estuary was cut off by construction projects in the 1930s, causing the basin to dry up for ~70 years. In 2005, a pilot channel was built to reconnect the estuary to tidal waters, allowing the basin to refill. However, the pilot channel, in addition to other barriers to water flow, do not allow for adequate tidal exchange, leading to intermittent, extreme hypersalinity (up to 180). Presumably because of the extreme hypersalinity in parts of the Bahia Grande, seagrass beds, which play vital roles in controlling community composition and driving biotic processes in estuaries, are not uniform throughout the estuary. Thus, this project aimed to develop salinity and seagrass distribution models for the Bahia Grande and to investigate changes in trace gas fluxes, macroinvertebrates, and fish community structure along those gradients.

DEDICATION

The completion of my master's work would not have been possible without the love and support of my family and friends. To my mother, Karen, my stepfather, David, my father, Randy, and my stepmother, Dawn – thank you for always supporting me and believing in me. To the old friends at home in Austin and to the new friends here in South Texas, thank you for both motivating and grounding me throughout this process.

ACKNOWLEDGMENTS

Most of all, I would like to express my sincerest gratitude to Dr. David Hicks for his seemingly never-ending support and guidance throughout this process. I would also like to extend my thanks to the rest of my committee members: Dr. Alejandro Fierro and Dr. Abdullah Rahman for helping me learn and grow as a student, scientist, and data analyst. Although not part of my committee, I would also like to thank Dr. Erin Easton, Dr. Eric Chan, and Leticia Contreras for their willingness to sacrifice their time to ensure my work was of the highest caliber. I truly appreciate each one of you.

I would also like to thank my fellow graduate students and other associates who volunteered to help with data collection and processing: Doug Faircloth, Chelsea Pavliska, Stefany Salinas, Jim Stilley, Mario Molina, and Gus Plamann. To the University employees who do so much for each one of us behind the scenes: Guillermo Aguilar and Skye Zufelt, thank you for your time and dedication to each and every student.

Most importantly, I would like to thank Friends of Laguna Atascosa National Wildlife Refuge for not only making this work possible, but also making it a priority. These thanks extend to all of the professionals I had the pleasure of working with through the U.S. Fish and Wildlife Service: Roy Ulibarri, Boyd Blihovde, and Sara Miller, thank you to each one of you for guiding me throughout this process and always being willing to provide a helping hand.

TABLE OF CONTENTS

LIST OF TABLES

Page

LIST OF FIGURES

Page

CHAPTER I

INTRODUCTION & LITERATURE REVIEW

The Bahia Grande is a 6,500-acre tidal basin located at the southernmost tip of Texas and is the largest of three water basins (i.e., Bahia Grande, Little Laguna Madre, and Laguna Larga) that comprise the Bahia Grande Unit of the Laguna Atascosa National Wildlife Refuge (Figure 1). A variety of tidally influenced habitats, including shallow open-bay bottom, seagrass meadow, and extensive tidal flats are found in the Bahia Grande Unit (Hicks et al. 2010). It historically functioned as an important nursery area for a variety of fish species and provided valuable habitat for wintering waterfowl and other birds (Hicks et al. 2010; Figure 1a).

A surveyor's map from 1884 shows that the Bahia Grande was connected to the Laguna Madre and nearby bays and may have even received freshwater input from San Martin Lake (Figure 2). However, due to the placement of dredged sediment during construction of the Brownsville Ship Channel in the 1930s, the natural tidal exchange between the Bahia Grande and the Laguna Madre was substantially reduced. The construction of State Highway 48 in the mid-1940s further reduced the tidal flow, causing the three basins to dry up and remain so for nearly 70 years (Figure 1b). The dried basins became a source of blowing sand that negatively affected surrounding vegetation and nearby residential communities, including Port Isabel, Laguna Heights, and Laguna Vista (USFWS 2004).

In an attempt to restore the Bahia Grande as a healthy estuarine ecosystem, a passive restoration strategy was implemented in 2005 when a 4.5 m (15 ft) wide, 685.5 m (1,250 ft) long

pilot channel was built to connect the Brownsville Ship Channel to the Bahia Grande (Hicks et al. 2010). The wetland soon refilled, alleviating the blowing sand and allowing fish to return to the estuary (Figure 1c). In 2007, two internal channels were built to reconnect the Bahia Grande to the two smaller basins of Laguna Larga and Little Laguna Madre (Hicks et al. 2010). Because of the size of the current pilot channel, only 3% of the water in the Bahia Grande is exchanged per tidal cycle (Hicks et al. 2010). This inadequate tidal exchange in the Bahia Grande leads to intermittent, extreme hypersalinity with values ranging from 35 near the inlet channel to values over 150 in northern areas farthest away from the inlet channel (Hicks et al. 2010). Thus, the Bahia Grande is considered a negative estuary, with inverse salinity trends (i.e., salinities are lowest at the inlet and increase farther away from the inlet), relative to the majority of coastal estuaries with salinities of 0 at the mouth of a river to 35 near their confluence with the ocean.

Although salinity gradients are characteristic of coastal estuaries, few estuaries worldwide experience such extreme hypersalinity as the Bahia Grande. Other hypersaline estuaries and bays typically have peak salinities around 60 to 70 that vary seasonally. The extreme hypersalinity of the Bahia Grande is the result of a variety of factors, including inadequate circulation, long water residence times, a high surface area to volume ratio resulting in high evaporation rates (i.e., little yearly rainfall and high temperatures), and barriers to water flow (e.g., historical railroad trestle and cattle fences; Hicks 2010). In addition, the Bahia Grande has little to no freshwater input from sources other than direct precipitation, and thus salinities are highly variable along the length of the estuary and are often dependent upon seasonal climatic variability (Hicks et al. 2010). Further rehabilitation plans include the construction of a 45.5 m (150 ft) wide permanent channel to replace the pilot channel to improve

water circulation, likely resulting in a more typical salinity range. In estuarine systems, salinity is the principal environmental factor in defining the communities of aquatic organisms (e.g., fish and macroinvertebrates) within the system (Barletta et al. 2005, Maes et al. 1998, Martino & Able 2003, Sosa-Lopez et al. 2007, Telesh & Khlebovich 2010, Vega-Candejas & Santillana 2004, Velasco et al. 2004, Waterkeyn et al. 2008). Thus, a shift to more typical salinity ranges will further support the rehabilitation of the estuarine system as a nursery habitat for a variety of biota (Cornejo 2009, Hicks et al. 2010). To evaluate its rehabilitation, it is important to establish baseline conditions and monitor changes in biotic communities in response to the effects of rehabilitation efforts (e.g., changes in salinity).

Despite being one of the largest wetland rehabilitation efforts in the United States, little research has been conducted in the Bahia Grande. No historical data exists that describes conditions in the Bahia Grande prior to the construction of the Brownsville Ship Channel and Highway 48 in the early-to-mid 1900s (i.e., before the basin dried up). The limited research conducted in the Bahia Grande after reflooding has revealed that salinity variations within the basin affect fish assemblages, decomposition rates, and barnacle development. Cornejo (2009) showed that variations in salinity between the northern and southern portions of the Bahia Grande explained a significant amount of spatial and temporal variation in fish assemblages, and that the value of the Bahia Grande as a nursery habitat for juvenile fishes is significantly diminished under such a widely fluctuating salinity regime. Marquez et al. (2017) found that leaf litter decomposition rates were significantly slower in the north Bahia Grande than in the south Bahia Grande, likely due to the lack of water flow and higher salinities found in the northern portions of the basin. In addition, decomposition rates in the south Bahia Grande were not significantly different from the nearby, healthy reference site, South Bay, indicating that

ecosystem functioning in the southern portion of the Bahia Grande resembles that of a healthy ecosystem (Marquez et al. 2017; Figure 1b, 1c). In addition, Martinez et al. (2015) showed that barnacle recruitment and growth trends were not significantly different in the south Bahia Grande and South Bay, further supporting the idea that the southern portion of the Bahia Grande resembles healthy conditions in nearby reference sites. Although these studies have identified salinity effects between the northern and southern Bahia Grande, none of the studies have directly quantified the salinity gradient and its effects across the entire estuary.

In addition to the effects of salinity on various structural and functional metrics, seagrasses also play vital roles in controlling community composition and driving biotic processes in estuaries (Attrill et al. 2000, Connolly 1994, Gray et al. 1996, Houte-Howes et al. 2004, Jackson et al. 2001, Mills & Berkenbusch 2009, Orth et al. 1984). Upper and lower temperature and salinity tolerance limits determine where seagrasses are able to establish and survive (McMahan 1968, McMillan & Moseley 1967). *Halodule wrightii*, the first recorded and only seagrass species currently present in the Bahia Grande, was shown to grow at salinities in excess of 60 but die after 28 days at salinities in excess of 70 (McMahan 1968, McMillan & Moseley 1967). Presumably due to the extreme hypersalinity (> 70) found in the northernmost part of the Bahia Grande, most *H. wrightii* seagrass beds are found closer to the inlet channel and gradually decline farther away from the channel (pers. obs.). Much like the salinity gradient, the distribution of seagrasses in the Bahia Grande has important implications for estuarine biota, processes, and rehabilitation.

Because it has been 14 years since reflooding, the Bahia Grande has reached a new steady state as it is unlikely that conditions will change significantly any further until the opening of the permanent channel, which is expected to result in substantial changes to this ecosystem.

Thus, it is imperative to characterize the salinity and seagrass gradients that exist within the estuary and to determine their direct effects on various estuarine biota and processes prior to the construction of this channel.

Trace Gas Fluxes

Trace gases are gases in the atmosphere that comprise less than 0.1% (NOAA 1996). Despite the relatively small contribution of trace gases to the overall composition of the atmosphere, several trace gases are of particular importance due to their radiatively active nature (NOAA 1996). Radiatively active gases are gases that absorb or emit atmospheric radiation and thus contribute to global climate warming. Of the radiatively active gases in our atmosphere, methane (CH_4) and carbon dioxide (CO_2) are two of the most important contributors to climatic warming (NOAA 1996). Although estuaries are thought to be effective ecosystems for reducing radiative effects through the uptake and burial of CO_2, these ecosystems can also release large amounts of CH_4, a gas with 25 times (over a period of 100 y) the radiative potential of CO_2, through the decomposition of organic matter (Magenheimer et al. 1996, Sun et al. 2013). Although estuaries comprise a mere 0.4% of ocean area, they contribute 7.4% of the total oceanic methane emission, which will likely increase if anthropogenic perturbations continue (Bange et al. 1994; Purvaja & Ramesh 2001). Thus, fluxes of CO_2 and CH_4 gases between estuaries and the atmosphere are of particular importance.

In estuaries, a complex relationship exists among salinity, dissolved sulfate concentration, and fluxes of CO_2 and CH_4. In typical positive estuaries where salinity ranges from 0-35, there is a strong negative correlation between salinity and both CO_2 and CH_4 efflux (Amouroux et al. 2002, Angelis & Lilley 1987, Bartlett et al. 1987, Huang et al. 2015, Nyman & DeLaune 1991, Purvaja & Ramesh 2001, Upstill-Goddard et al. 2000, Smith et al. 1983). The

decline in CH_4 emissions at higher salinities (~35) is likely due to the inhibitory effects of high salinity on the activity of methanogens, or methane producing bacteria (Zeng et al. 2008). Studies have also shown that the efflux of CO_2 in estuaries is lower in high salinities areas (~35) than freshwater areas (Frankignoulle et al. 1998, Huang et al. 2015, Nyman & DeLaune 1991, Smith et al. 1983). Sulfate, an anion naturally found in seawater, is typically found in higher concentrations in areas of estuaries receiving more tidal input. The effects of sulfate on trace gas emissions in estuaries ranging from 0-35 are similar to the effects of salinity, with increasing sulfate concentration leading to lower CO_2 and CH_4 efflux (Magenheimer et al. 1996, Van Horn et al. 2014). Sulfate, like salinity, not only restricts the process of methanogenesis, but also acts as the primary electron acceptor during respiration in anoxic sediments, limiting the decomposition of organic matter (Howarth 1984). Thus, areas with higher dissolved sulfate concentrations, due to increased tidal flushing, have lower CO_2 and CH_4 emissions (Angelis & Lilley 1987, Magenheimer et al. 1996, Purvaja & Ramesh 2001, Poffenbarger et al. 2011). The effects of salinity and sulfate on trace gas efflux in estuaries ranging from 0-35 are additive, with an increase in both leading to lower CO_2 and CH_4 efflux.

The relationship between salinity and sulfate and their effects on trace gas fluxes in negative estuaries like the Bahia Grande is less well understood. In negative estuaries, high salinity areas (>35) often do not receive much tidal input and therefore sulfate. Thus, the effects of salinity and sulfate concentration on trace gas fluxes become confounding in negative estuaries as opposed to additive in positive estuaries. The specific salinity and sulfate concentration at which trace gas emissions increase or decrease in estuaries remains largely unknown. It is also unknown whether salinity or sulfate concentration has a more dominant control over trace gas emissions in estuaries. Thus, the Bahia Grande provides a unique

opportunity to understand the relationship between extreme salinities, sulfate concentrations, and CO_2 and CH_4 emissions and to determine whether inadequate flushing in this partially restored estuary affects these fluxes.

Wetland plants can also affect CO_2 and CH_4 emissions because they provide effectual pathways for the diffusion of trace gases between the sediment and the atmosphere (Bouillon et al. 2007, Purvaja & Ramesh 2001). For example, several studies have shown that significantly higher fluxes of CO_2 and CH_4 occur in areas with dense seagrass beds than in bare sediment areas (Barber & Carlson 1993, Magenheimer et al. 1996). Although the above-ground portion of seagrasses acts as a pathway for gas efflux to the atmosphere, the below-ground biomass allows for high levels of carbon sequestration. For example, McKee et al. (2007) showed that seagrass meadows in the Caribbean had carbon deposits 10 m thick and over 6000 years old. Seagrasses trap large amounts of suspended matter from the water column or atmosphere in their roots and sequester the organic carbon that is produced as a result of high levels of primary production (Mcleod et al. 2011, Russell et al. 2013). The loss of these carbon-sequestering seagrass habitats significantly reduces the capacity of a system for long-term carbon storage by accelerating erosion and leading to the leaching of dissolved carbon (Mcleod et al. 2011). In addition, the loss of native seagrasses often leads to recolonization by seagrass species with lower capacities for carbon sequestration (Mcleod et al. 2011). However, successful restoration efforts often allow seagrasses to recolonize and succession to occur so that seagrass species with higher capacities for carbon sequestration can dominate the estuary. For example, Marba et al. (2015) showed that seagrass revegetation fully restores the capacity of a system to sequester carbon through carbon deposition and burial in as little as 18 years following revegetation.

The Bahia Grande provides a unique opportunity to explore CO_2 and CH_4 flux patterns under hypersaline conditions, as these patterns have generally only been studied in estuaries with salinities < 35. In addition, conditions in the Bahia Grande allow for an exploration of the relationship between trace gas fluxes, the carbon and nitrogen content of the sediment, and the presence/absence of seagrasses in areas of similar salinity. Documenting these patterns prior to the next restoration phase (i.e., construction of the larger, permanent channel) is vital to understanding the impact of future restoration efforts. In addition, these findings can be used to inform rehabilitation efforts in other estuaries that were formerly dried and now have limited tidal flow.

Fish Community Structure

Estuarine habitats represent an important nursery area for many fish species that utilize estuaries to feed, grow, or spawn. The fishes that reside within estuaries play an important role not only in the export of nutrients from coastal areas to the marine ecosystem, but also in the maintenance of ecosystem processes through their role in trophic relationships (Sosa-Lopez et al. 2007). Estuaries also represent an important source of fishes for human recreation and consumption.

A variety of biotic (e.g., competition, predation) and abiotic (e.g., salinity, temperature, habitat availability) factors can affect the structure and distribution of fish communities within an estuary. Of these factors, salinity has been shown to be the most important determining factor of fish distribution, abundance, species richness, and species diversity in estuaries (Akin et al. 2003, Barletta et al. 2005, Maes et al. 1998, Martino & Able 2003, Rakocinski et al. 1992, Vega-Candejas & Hernandez de Santillana 2004). Salinity gradients act as a continuum of stress (i.e., osmotic stress) for fish, causing them to migrate throughout estuaries in response to differences

in salinity (Akin et al. 2003, Barletta et al. 2005). Osmotic stress is especially prevalent at extremely high (> 60) or low (< 12) salinities because of differences between the internal osmotic regulatory mechanisms of fish and the surrounding environment (Martino & Able 2003, Vega-Candejas & Hernandez de Santillana 2004). Thus, the changes in salinity that occur along an estuary can act as a physical barrier to the movement and survival of various fish species, diminishing the value of the estuary as a nursery for estuarine-dependent juvenile fishes.

Although many scientific studies on estuarine fish communities were conducted in estuaries ranging from 0 to 35, relatively few have focused on hypersaline estuaries. Of the studies conducted in hypersaline estuaries, most found a strong negative correlation between salinity and fish species diversity, abundance, and richness (Sosa-Lopez et al. 2007, Vega-Candejas & Hernandez de Santillana 2004). Thus, fish community structure in lower salinity areas of hypersaline estuaries is largely determined by biotic factors (e.g., competition, predation), whereas abiotic factors (e.g., salinity, temperature) shape community structure at higher salinities (Vega-Candejas & Hernandez de Santillana 2004). For example, Vega-Candejas & Hernandez de Santillana (2004) found relatively high species richness and low abundance at salinities of ~35 (near the inlet of the estuary), high species richness and high abundance at 50-60, and low species richness and low abundance at 70-110 (Vega-Candejas & Hernandez de Santillana 2004). Under extreme hypersaline conditions (> 70), species richness decreases, diminishing the amount of competitive interactions, whereas species richness and competition are high under marine conditions (~35; Vega-Candejas & Hernandez de Santillana 2004). The extreme variations in salinity throughout hypersaline estuaries like the Bahia Grande make them optimal habitats for communities of salt-tolerant, resident forage fishes but generally unsuitable for transient juveniles that are unable to tolerate large variations in salinity (Vega-

Candejas & Hernandez de Santillana 2004). Thus, prolonged hypersalinity in an estuary prevents the estuary from serving its purpose as a nursery for a variety of fish species. Such patterns are consistent with Cornejo's (2009) findings that fish communities in the Bahia Grande were heavily dominated by one species (*Cyprinodon variegatus*) and that fish community richness and diversity was lowest in the northern areas of the basin where salinities were the highest.

In addition to the effects of salinity on fish communities, seagrasses also play an important role in shaping biotic assemblages within estuaries. Seagrass beds are particularly important for fish species because they act as permanent habitats, temporary nurseries, feeding areas, and provide refuge from predation (Gray et al. 1996, Jackson et al. 2001). The absence of this important habitat for fish can limit their distribution regardless of water quality (Maes et al. 1998). Areas with higher seagrass coverage tend to provide more habitat heterogeneity, leading to higher fish species richness and diversity in seagrass beds than in bare areas (Arrivillaga & Baltz 1999, Connolly 1994, Gray et al. 1996, Vega-Candejas & Hernandez de Santillana 2004). Thus, areas in the Bahia Grande with lower salinities and higher amounts of seagrasses are likely to have higher fish species richness and diversity.

Macroinvertebrate Community Structure

Benthic macroinvertebrates (e.g., mollusks, crustaceans, polychaetes) are often used as indicators of the severity of environmental degradation in estuaries due to the high susceptibility of certain taxa to environmental stress (Wildsmith et al. 2011). While a variety of stressors can lead to changes in macrobenthic communities, salinity has been shown to be the most important determining factor of macroinvertebrate community composition in estuaries (Mannino & Montagna 1997, Velasco et al. 2006). A negative correlation exists between salinity and

macroinvertebrate richness and diversity in estuaries (Brucet et al. 2012, Velasco et al. 2006, Waterkeyn et al. 2008). However, Velasco et al. (2002) showed that significant changes in community composition only occurred once salinities exceeded 75, below which occasional changes in salinity did not significantly affect community structure. In addition, Mannino & Montagna (1997) showed that macrobenthos diversity is the lowest in areas where changes in salinity occur most rapidly over a short distance. Thus, hypersalinity and other ecological disturbances (e.g., pollution) can lead to the disappearance of many species and the dominance of a few tolerant species (Kefford 2000, Williams 1999). Tamez (2014) showed that polychaete communities in the Bahia Grande are dominated by few species and have low diversity when compared to nearby reference sites. A survey of macrobenthos in the Bahia Grande will determine if changes in macrobenthic community structure occur along a hypersaline gradient and will provide critical baseline data to monitor the restoration status of the estuary after construction of the permanent channel.

The effect of salinity on macroinvertebrate structure is largely due to differences in habitat (e.g., seagrass presence/absence) rather than by osmoregulatory limitations (Verschuren et al. 2000). For example, the abundance, diversity, and species richness of macroinvertebrates is significantly higher in areas with uniform seagrass beds than in areas with fragmented seagrass patches and/or no seagrass, likely due to the protection from predators that seagrass beds provide (Arrivillaga & Baltz 1999, Houte-Howes et al. 2004, Mills & Berkenbusch 2009, Peterson 1982). In addition, the aboveground biomass of seagrasses is significantly positively correlated with benthic macroinvertebrate richness and abundance (Attrill et al. 2000, Heck & Wetstone 1977). For example, Attrill et al. (2009) showed that the biomass of seagrass beds, opposed to the structural complexity or diversity of plant species, was responsible for the increase in the

richness and diversity of macroinvertebrate communities. Thus, areas of the Bahia Grande with lower salinities and higher seagrass coverage are expected to have higher macroinvertebrate species richness and diversity than areas with higher salinities and lower seagrass coverage.

Objectives/Hypotheses

Because the salinity gradient, seagrass distribution, and their effects on trace gas fluxes, fish community structure, and macroinvertebrate community structure have not been explored in the Bahia Grande, the effects of preliminary restoration efforts (e.g. construction of the pilot channel) have not been fully assessed. With the upcoming construction of the permanent channel, understanding these patterns and relationships are of particular importance to provide a baseline for assessing the effectiveness of future restoration efforts. To understand these patterns and provide the necessary baseline data, this study collected trace gas flux, macrobenthos, and fish data along salinity and seagrass gradients in the Bahia Grande.

Because of the extreme hypersalinity throughout much of the Bahia Grande and the expected effect of salinity and seagrass abundance on trace gas fluxes, fish community structure, and macroinvertebrate community structure, I hypothesize that (1) CO_2 and CH_4 fluxes will (a) decrease as salinity increases and (b) increase as seagrass coverage increases; (2) fish species richness and diversity will (a) decrease as salinity increases and (b) increase as seagrass coverage increases; and (3) benthic macroinvertebrate richness and diversity will (a) decrease as salinity increases and (b) increase as seagrass coverage increases. To substantiate these hypotheses, the following objectives were executed: (1) generate salinity and seagrass gradient maps; (2) measure fluxes of CO_2 and CH_4 along established salinity and seagrass gradients; (3) document benthic community structure along salinity and seagrass gradients; and (4) document fish community structure along salinity and seagrass gradients.

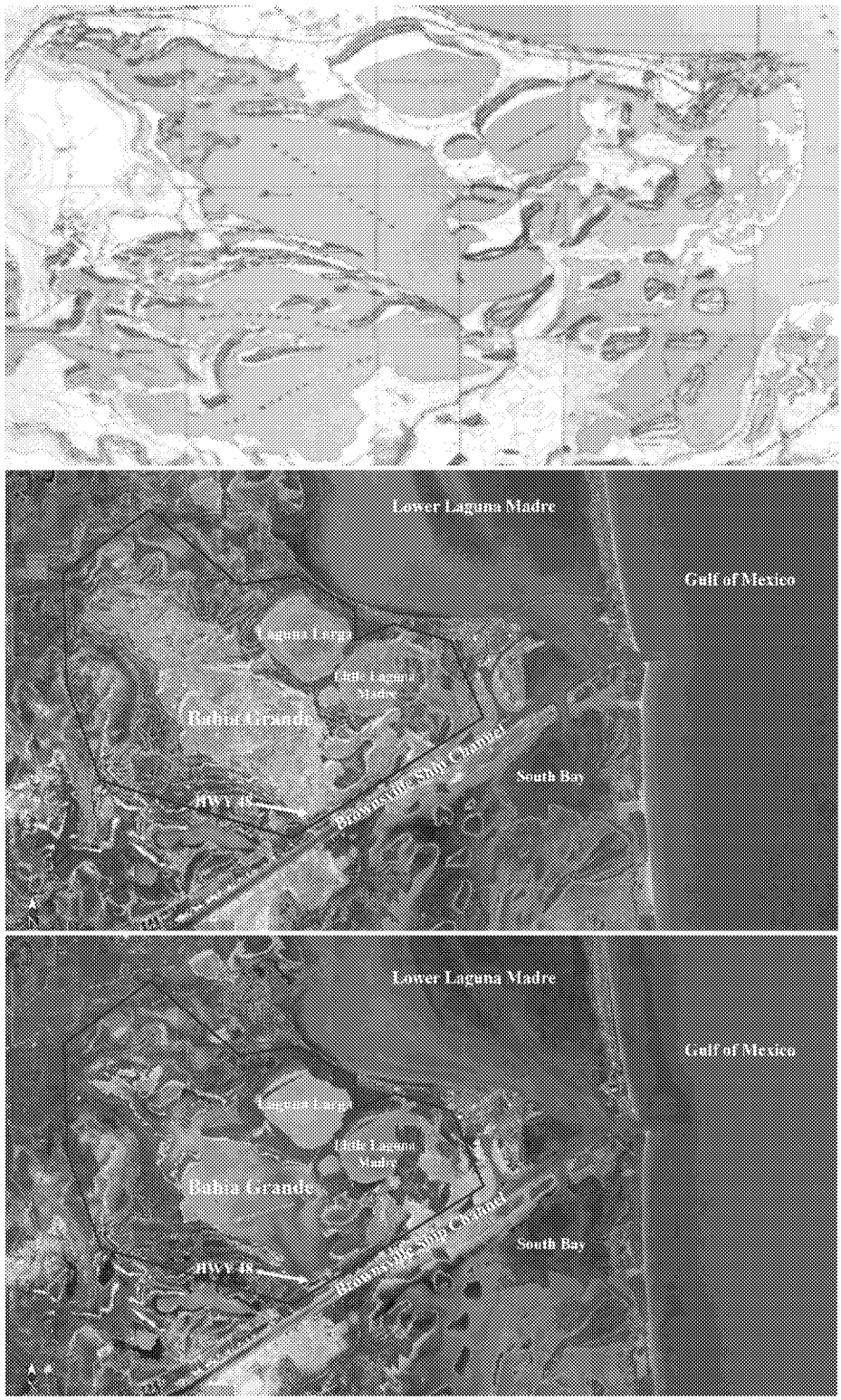

Figure 1 (a-c). Depiction of Bahia Grande Unit pre-1930s (a), and Google Earth Images of the Bahia Grande in December 1990 before reflooding (b) and in December 2017 after reflooding (c). Red outlines in (b) and (c) indicate the border of the Bahia Grande Unit of the Laguna Atascosa National Wildlife Refuge.

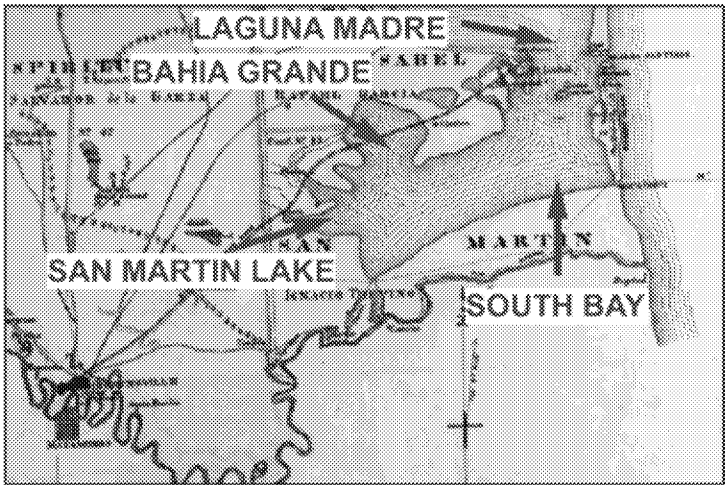

Figure 2. Surveyor's map of the Bahia Grande and surrounding bays from 1884 (Lichlyter 2006). Originally from J.J. Cocke, Map of the County of Cameron, Texas, October 25, 1884.

CHAPTER II

METHODOLOGY

Study Site

The Bahia Grande is a tidal basin located within the Laguna Atascosa National Wildlife Refuge in South Texas. The estuary is hypersaline (>70) during periods of low rainfall and high temperatures due to its restricted tidal inflow, large surface area (>25 km^2), and shallow depths (<1 m; Hicks et al. 2010). In addition to the size of the pilot channel allowing only 3% tidal exchange for the Bahia Grande, a historic railroad trestle dividing the basin into northern and southern areas also potentially limits circulation (Hicks et al. 2010, USFWS 2004). Algal mats cover a majority of the seafloor, and seagrasses (*H. wrightii*) have established in some parts of the estuary in the last six to seven years (Hicks et al. 2010, pers. obs.). Oyster beds and black mangroves are found fringing the shoreline near the channel inlet (Tamez 2014). Sediment composition ranges from areas that are primarily silt, to areas that are primarily clay with only minimal amounts of silt and sand (Hicks et al. 2010). Wind speeds on the water tend to be higher than surrounding areas due to the openness of the basin (pers. obs.). The southern area of the Bahia Grande (i.e., area south of the railroad trestle that receives the majority of the tidal exchange) has been shown to resemble the typical features of a reference site (i.e., South Bay; Marquez et al. 2017, Martinez 2015), and therefore may serve as the reference site for the northern areas of the Bahia Grande (i.e., areas north of the railroad trestle that receive little to no tidal exchange) in this project.

Salinity Gradient Mapping

Salinity data was collected at 71 sites (34 sites in the southern area, 37 sites in the northern area) across the Bahia Grande on 23 July 2019 under typical conditions for the estuary (i.e., no recent rainfall events; Figure 3). At each site, a Hydrolab Compact DS5 multi-parameter probe (Hydrotech ZS, Round Rock, TX, USA) was used to collect environmental data, including salinity (from specific conductivity), water temperature, dissolved oxygen, pH, and chlorophyll a. In areas where the salinity was too high to be determined with the data sonde, water samples were taken and returned to the lab, where they were diluted 1:1 with deionized water and the salinity was determined with a refractometer. A Trimble Juno 3B was used to record the GPS location at each sampling site (Sunnyvale, CA, USA). The GPS coordinate data files recorded by the Trimble Juno 3B for each site were imported into GPS Pathfinder Office software and differentially corrected using the nearest base station in order to improve the accuracy of each GPS position. The corrected GPS locations and corresponding salinity values were imported into ArcMap, where gradients were mapped using the kriging tool in the Geostatistical Analyst toolbox. All default parameters were selected. The kriging interpolation method estimates values at unknown points based on values at known points using Gaussian processes. Each value is then assigned to a given class based on natural breaks in the data (e.g., 0-20, 20-40, 40-60). A temperature distribution map was also generated according to the methods above using the temperature values collected at 71 sites during salinity sampling. This map is simply a visual representation of the temperature gradient in the Bahia Grande and was not utilized for analyses.

Seagrass Distribution Mapping

In order to determine seagrass coverage throughout the Bahia Grande, WorldView-2 (WV-2) imagery taken on December 16, 2018 was purchased from Harris Geospatial. The

WV-2 satellite sensor provides panchromatic imagery with a resolution of 0.46 m and eight-band (red, green, blue, coastal, yellow, red-edge, 2 near-infrared) multispectral imagery with a resolution of 1.84 m.

The orthorectified 8-band multispectral WV-2 image was imported into ERDAS Imagine version 16.1 software (Hexagon Geospatial, Madison, AL, USA) for all data analyses. The eight layers (i.e., one layer per band) were stacked. The stacked image was converted from radiometrically corrected image pixel values (i.e., digital numbers) to band-integrated radiance using Equation 1, where $L_{Pixel,Band}$ is the top-of-atmosphere band-integrated radiance image pixels, $absCalFactor_{Band}$ is the absolute radiometric calibration factor for a give band provided in the metadata file, and $q_{Pixel,Band}$ is the radiometrically corrected image pixels.

Equation 1. $$L_{Pixel,Band} = absCalFactor_{Band} \times q_{Pixal,Band}$$

After the image pixels were converted to band-integrated radiance, the top-of-atmosphere, band-averaged, spectral radiance image pixels were calculated using Equation 2, where $L_{\lambda Pixel,Band}$ is the top-of-atmosphere band-averaged spectral radiance image pixels, $L_{Pixel,Band}$ is the top-of-atmosphere band-integrated radiance image pixels, and $\Delta\lambda_{Band}$ is the effective bandwidth for a given band provided in the metadata files.

Equation 2. $$L_{\lambda Pixel,Band} = \frac{L_{Pixel,Band}}{\Delta\lambda_{Band}}$$

The solar zenith angle was then calculated using Equation 3, where θ_s is the solar zenith angle and *sunEl* is the sun elevation provided in the metadata files.

Equation 3. $$\theta s = 90.0 - sunEl$$

The image was then converted to top of atmosphere band-averaged reflectance using Equation 4, where $\rho_{\lambda Pixel,Band}$ is the target diffuse spectral reflectance, $L_{\lambda Pixel,Band}$ is the top of atmosphere band-averaged spectral radiance, d_{ES} is the Earth-Sun distance equal to 1 AU, $Esun_{\lambda Band}$ is the band-

averaged solar spectral irradiance normal to the surface being illuminated provided in Digital Globe document), and θ_s is the solar zenith angle.

Equation 4. $$\rho_{\lambda \text{Pixel,Band}} \frac{L_{\lambda \text{Pixel,Band}} \bullet d_{ES}{}^2 \bullet \pi}{Esun_{\lambda \text{Band}} \bullet \cos(\theta s)}$$

Once the image pixels were converted to top of atmosphere band-averaged reflectance, the "Signature Editor" was used to create a spectral signature set by drawing polygons around the 71 areas with ground-truth seagrass coverage data. Each polygon was classified as "Dense" (i.e., seagrass coverage of 67-100%), "Moderate" (i.e., seagrass coverage of 34-66%), or "Bare/Sparse" (i.e., seagrass coverage of 0-33%) based on the seagrass coverage estimates and GoPro videos collected at 71 sites during salinity sampling. Data classification of the image was conducted using the supervised classification tool with all default settings, which uses the spectral signature set previously created to classify all pixels within the image into one of the three predetermined classes (i.e., dense, moderate, bare/sparse).

Trace Gas Flux Measurements

Trace gas fluxes were measured at 18 sites approximately equidistant apart along the salinity gradient map established in ArcGIS by drawing a line from the sampling site with the lowest salinity to the sampling site with the highest salinity (Figure 4). Sites in the northernmost portion of the basin were excluded as these areas are shallow tidal flats where inundation is episodic and largely dependent on windspeed and direction (i.e., too shallow to utilize benthic chambers). In situ measurements of the concentrations of dissolved trace gases (i.e., CO_2 and CH_4) in the water column were taken using a 10 L benthic chamber constructed from a Chemglass jar (Vineland, NJ, USA; Figure 5). Benthic chambers were inserted 5 cm into the sediment to prevent ambient water exchange during sampling and to ensure consistent chamber volume among samples. The chambers were connected to a Los Gatos Dissolved Gas Extraction

Unit (DGEU) and a Los Gatos Ultraportable Greenhouse Gas Analyzer (UGGA; Los Gatos Research, San Jose, CA, USA). A pump inside the chamber pumped water at 2 L/min into the gas extraction unit, where the gases were extracted from the water and sent to the gas analyzer (Figure 6). The extraction unit then returned the gas-free water to the chamber to prevent depletion of the water inside the chamber. The gas analyzer recorded CO_2 and CH_4 concentrations every 21 s for 5 min; concentrations could be viewed in real-time on an iPad or downloaded as an Excel spreadsheet. Environmental measurements, including water temperature, salinity (from specific conductivity), depth, turbidity, dissolved oxygen, pH, and chlorophyll a were collected using a Hydrolab Compact DS5 multi-parameter probe at each of the 18 sites.

In addition, water samples were collected from each of the 18 sampling sites for sulfate analysis. Water samples were collected in 250 ml plastic containers without preservative and kept on wet ice until they could be transferred to the laboratory. Water samples were maintained at 6°C or below until they were sent to A&B Labs (Houston, TX, USA) for sulfate analysis.

A cylindrical push corer (5.5 cm inner diameter) was used to collect two sediment cores to a depth of 4 cm from each of the 18 sampling sites to determine the carbon and nitrogen content of the sediments and their potential correlation with CH_4 and CO_2 fluxes. Samples were kept on wet ice until they could be transferred to the laboratory where they were frozen until processing could occur. Each frozen sample was cut into 2 cm increments by depth, yielding a total of four samples per site and 72 samples overall. A wet weight was recorded for each sample prior to drying. Samples were then placed in an oven at 60°C until they reached a constant weight (at ~72 h), at which point they were cooled and re-weighed to obtain a dry weight. Sediment samples were subsequently homogenized using a mortar and pestle and sieved

through a 125 μm sieve. To correct for inorganic carbon content, ~0.5 g of each sample was placed into a ceramic crucible and heated to 500°C until a constant weight was reached, at which point the samples were reweighed (i.e., "burned samples"). A Perkin Elmer 2400 CHNS/O Series II elemental analyzer was used to determine the percentage of total carbon and nitrogen content for each homogenized sample. Inorganic carbon content was determined using the following equation: Inorganic Carbon Content = Total Carbon Content of Burned Sample x (Dry Mass After Burning/Dry Mass Before Burning). Organic carbon content was then calculated by subtracting the inorganic carbon content from the total carbon content of the non-burned samples. The 0-2 cm and 2-4 cm subsections of each core were summed, and replicates were averaged prior to data analyses.

The flux rate of CO_2 and CH_4 at each site was calculated from changes in gas concentrations over time. Due to the sporadic initial trace gas readings obtained from the UGGA (i.e., first two minutes), data were reduced to the linear portion of the gas concentration vs. time curves (i.e., remaining three minutes) prior to linear regression analyses. Gas concentration vs. time coefficients were corrected to account for rates of gas removal from the chamber system by the DGEU and potential measurement drift by the UGGA under three experimental conditions: (1) saltwater with a salinity of 70 at 30°C, (2) saltwater with a salinity of 44 at 30°C, and (3) gas analyzer only (no extractor). The first two experimental conditions were used to determine the rate of gas extraction under conditions of varying salinity at the average water temperature of field measurements, while the third was meant to capture any drift of the gas analyzer in the absence of the extractor. Data from each experiment were reduced to the most consistent linear segment of the resulting concentration vs. time curve, and a linear regression of the change in gas concentration over time was calculated for CO_2 and CH_4 under all experimental conditions.

Because the respective rates of extraction (i.e., slopes of linear regression) of CO_2 and CH_4 under the first two experimental conditions (varying salinity) were within two standard deviations of one another, an average of the two slopes for both CO_2 and CH_4 was calculated and added to the slopes of the linear regressions for machine drift (i.e., one for CO_2 and one for CH_4). The resulting slopes were then added to the slopes of the linear regressions calculated for CO_2 and CH_4 data collected in the field.

The corrected concentration vs. time slope values from the field data were then converted from a concentration (i.e., ppm/sec) to a mass-based gas flux per unit area (i.e., micromole/m^2/sec) by accounting for the mass of all gases within the chamber at the time of sampling (Howard et al. 2014). The number of gas molecules in the chamber (n) was determined by the equation n = PV/RT, where P is the atmospheric pressure (i.e., 1 atmos), V is the volume of the chamber (L), R is the universal gas constant (0.0820 L*atmos/K*mol), and T is the temperature of the gas in Kelvins at the time of each measurement. To determine the mass-based flux of CO_2 and CH_4, the slope of the best-fit line for each gas at each site was multiplied by the corresponding number of gas molecules in the chamber at the time of measurement. The resulting number was then divided by the area of the chamber to determine the amount of CO_2 and CH_4 emitted per second per unit area (i.e., μmol/m^2/sec).

Fish Sampling

Fish sampling in the Bahia Grande was conducted according to methods determined by U.S. Fish and Wildlife Service. In brief, Google Earth was used to divide the Bahia Grande into 10 randomly numbered 60×60-second grids (Figure 7). Each of the 10 grids contained 144 5×5-second gridlets. Bag seines were used to sample odd-numbered grids and gill nets were used to sample even-numbered grids. The bag seine measured 18.3 m (60 ft) long by 1.8 m (6 ft) deep

and was constructed of 13 mm (0.50 in) stretched nylon multifilament mesh in the bag and 19 mm (0.75 in) stretched nylon multifilament mesh in the wings. Bag seines were pulled parallel to the shore for 15.2 m (50 ft), and a 12.2 m (40 ft) rope was strung between the two poles to ensure consistent sampling area among sites and replicates. Gill nets measured 61 m (200 ft) long by 0.9 m (3 ft) deep with 15.2 m (50 ft) sections of 76 mm (3 in), 102 mm (4 in), 127 mm (5 in), and 152 mm (6 in) stretched monofilament mesh. Within bag-seine sampling grids, five shoreline gridlets were randomly selected using the random points generator in ArcGIS, and four bag-seine hauls were conducted per gridlet. Fish collected in bag-seine hauls were bagged and frozen until identifications and total length measurements were completed. Within each gill net sampling grid, one gridlet was randomly selected and sampled three times for a duration of 4 h per soak, resulting in a total soak time of 12 h per gridlet. Fish collected in gill nets were identified down to the lowest possible taxon, measured for total length, and released. Environmental measurements, including water temperature, salinity, measured depth, temperature, and dissolved oxygen, were collected using a Hydrolab Compact DS5 multi-parameter probe at each sampling site.

Macrobenthos Sampling

To maintain uniformity among previous benthic data collections in the Bahia Grande, benthos were sampled in accordance with the methods of Tamez (2014). The Bahia Grande was stratified into three sectors (BG-South, BG-Northwest, BG-Northeast); from each sector, eight sampling sites were randomly selected to ensure adequate sampling of the system (24 sites total, sampled biannually; Figure 8). Benthic sampling sites were selected prior to each sampling event by overlaying a 5×5-second grid onto a map of the Bahia Grande and randomly selecting intersecting points of degrees, minutes, and seconds. Extra sites were generated in the case that

some randomly generated sites were inaccessible. A cylindrical push corer (9.5 cm inner diameter; Aquatic Research Instruments, Hope, ID, USA) was used to collect four replicate sediment cores to a depth of 10 cm at each sampling site. Biannual benthos sampling resulted in a total of 192 benthic samples at 48 individual sites. After collection, samples were placed into individual 500 μm polypropylene mesh bags. Samples were pre-sieved in the field and placed in a seawater and ice-filled cooler for storage until sampling was complete (<8 h). Once sampling was complete, samples were taken to the laboratory where they were frozen until sieving on a 500 μm mesh sieve. Once sieving was complete, samples were stored in 100% ethanol and stained with the protein stain Rose Bengal. Stained samples were sorted and macrobenthos were identified down to the lowest possible taxon. In addition, environmental measurements, including salinity (from specific conductivity), measured depth, secchi depth, and water temperature, were collected using a Hydrolab Compact DS5 multi-parameter probe at each of the 48 sites.

Statistical Analyses

Trace Gas Fluxes

Distance-based linear modeling (DISTLM, Primer-E version 7.0 software) was performed based on a permutational regression between trace gas fluxes and environmental variables to determine the effect of various environmental predictors (i.e., salinity, sulfate concentration, seagrass coverage, DO (mg/L), water temperature, depth, and % organic carbon and total nitrogen content of the sediment) on trace gas fluxes. Prior to analyses, Draftsman plots were generated from the environmental and trace gas data sets in order to evaluate data symmetry and correlations among variables, and no transformations were necessary. A Euclidian distance similarity matrix was then constructed from the multivariate gas flux data.

Environmental data were not normalized prior to DISTLM analyses as normalization is a standard part of the routine. For the linear modeling, AIC_c selection criterion was chosen as this measure best handles a small number of samples (N) relative to the number of predictor variables (v); using AIC_c is recommended when the ratio of N/v is less than 40, and in this case, N/v is 3 (i.e., 18/6). The Best selection procedure was chosen because it examines the value of AIC_c for all possible combinations of predictor variables. The output from the Best selection procedure provides the best model for each number of variables as well as a list of the overall 10 best models. In order to visualize the effect of the best predictor variables on CO_2 and CH_4 fluxes at each sampling site, a distance-based redundancy analysis (dbRDA, Primer-E version 7.0 software) was performed from the raw data set.

A multivariate analysis of similarities (ANOSIM, Primer-E version 7.0 software) was used to test for differences in trace gas fluxes based on area (i.e., north and south), which compares ranked similarities between and within groups. To test for differences in trace gases based on seagrass coverage, a shapefile containing x,y data (i.e., geographic location coordinates) of the 18 carbon and nitrogen sampling sites were overlaid onto the seagrass classification map generated in ERDAS Imagine. Each sampling site was grouped into one of the three classes representing seagrass coverage (i.e., dense, moderate, bare/sparse) based on its location on the classification map. Due to the unequal number of samples categorized into each seagrass coverage group (i.e., dense, moderate, and bare/sparse), differences in trace gas fluxes based on seagrass coverage were tested for using a permutation-based analysis of variance (PERMANOVA, Primer-E version 7.0 software), which better handles discrepancies in sampling size among groups. Differences in trace gas fluxes based on sampling date (i.e., August and September) and time of day (8-10am, 10-12pm, 12-2pm, 2-4pm) were also tested for using

PERMANOVA analyses. Type III (partial) sum of squares and unrestricted permutation of raw data settings were selected for all PERMANOVAs, which are recommended for unbalanced one-way analyses. Lastly, a model matrix was created from latitude and longitude of trace gas samples, and a RELATE analysis was performed to examine the relationship between trace gas fluxes and geographic position, which compares the ranked similarities of the trace gases resemblance matrix to that of the model matrix (RELATE, Primer-E version 7.0 software).

In addition to including the percent organic carbon and nitrogen content of the sediment in the distance-based linear modeling, differences in sediment content based on sampling site were also investigated. Prior to analyses, Draftsman plots were generated from the environmental and carbon/nitrogen data sets in order to evaluate data symmetry and correlations among variables. Both data sets were normalized prior to analyses, and a Euclidian distance similarity matrix was then constructed from the multivariate carbon and nitrogen data set. To determine differences in sediment organic carbon and nitrogen content in southern and northern regions, data were analyzed using an ANOSIM. A non-metric multidimensional scaling analysis (nMDS, Primer-E version 7.0 software) was used to visualize the similarities among organic carbon and nitrogen based on area. Two-dimensional bubbles were overlaid onto the MDS-plot to show the relationship between salinity and organic carbon and nitrogen at various sites. Next, a model matrix was created from latitude and longitude of carbon and nitrogen samples, and a RELATE analysis was performed to examine the relationship between organic carbon and nitrogen and geographic position. This analysis compares the ranked similarities of the species abundance resemblance matrices to those of the model matrices. If the relationships between samples agree entirely between the sample and model resemblance matrices, then the rank correlation is equal to 1. The organic carbon and nitrogen data and environmental

ordinations of samples were compared using a Biotic and Environmental linking analysis (BIOENV, Primer-E version 7.0 software), resulting in combinations of environmental variables that are highly correlated with the ordination of carbon and nitrogen samples.

To test for differences in organic carbon and nitrogen content based on seagrass coverage, the previously grouped sampling coordinates (i.e., into bare/sparse, moderate, dense classes) and previously created design matrix (i.e., based on factor identifier for seagrass) were compared using a PERMANOVA, which was selected because of the unequal number of samples within each group. Type III (partial) sum of squares and unrestricted permutation of raw data settings were selected. To visualize differences in percent organic carbon and nitrogen content at 0-2 cm and 2-4 cm, site replicates at each depth were averaged and the resulting numbers were plotted on a graph. Lastly, a shapefile containing x,y,z data (i.e., longitude, latitude, and % organic carbon and nitrogen content) of the 18 sampling sites was overlaid onto the seagrass classification map generated in ERDAS Imagine. The graduated symbols tool, which assigns values to a given class based on natural breaks in the data (e.g., 0-1, 1-2, 2-3), was used to visualize differences in percent organic carbon and nitrogen content based on seagrass coverage.

Fish & Macroinvertebrate Community Structure

Species abundance data for the 83 fish sampling sites were standardized to make bag seine and gill net samples comparable, and species abundance data for the 192 macroinvertebrate subsamples were summed according to site (Standardize, Sum, Primer-E version 7.0 software). Shade plots were created from the fish and macroinvertebrate data and analyzed to determine the relative species contributions to subsequent analyses. Shade plots are simply a visual representation of the data matrix in which the contribution of each variable is represented by a

shade of grey (i.e., white is absent, black is largest worksheet value). If a few samples are black, while the rest are light gray or white, then a transformation is required in order to prevent the analyses from being dominated by only a few samples. While fish samples did not require transformation, macroinvertebrate samples were square root transformed prior to analyses. Fish samples were grouped according to geographic location into three areas (i.e., BG-S, BG-NE, BG-NW) to maintain consistency with macroinvertebrate sample grouping.

A Bray-Curtis similarity matrix was constructed from each data set. Because there was an unequal number of fish samples within each area, a one-way PERMANOVA, which better handles unbalanced sampling designs, was chosen to determine differences in fish communities among the three areas. Prior to PERMANOVA analysis, a design matrix was formulated from the factor identifier for area (fixed factor) to compare fish communities among BG-S, BG-NE, and BG-NW. Type III (partial) sum of squares and unrestricted permutation of raw data settings were selected, which are recommended for unbalanced one-way ANOVA analyses. The large number of samples (i.e., 83) prevented the use of a non-metric multidimensional scaling analysis (nMDS) due to high stress values. Thus, a metric multidimensional scaling analysis (mMDS, Primer-E version 7.0 software) was performed from the similarity matrix based upon 100 bootstrap averages from each area to visualize the similarities among fish samples in the three groups.

Unlike the fish data, the macroinvertebrate data had an equal number of samples within each area and thus did not require a more powerful PERMANOVA analysis. Instead, differences in macroinvertebrate communities based on area were compared using a one-way ANOSIM. The fewer number of macroinvertebrate samples (i.e., 48) allowed for the use of an nMDS to visualize the similarities among macroinvertebrate samples based on area. Two-dimensional

bubbles were overlaid onto the nMDS-plot to show the relationship between salinity and benthic invertebrate abundance at various sites. Separate PERMANOVA (fish) and ANOSIM (macroinvertebrate) analyses were used to test for differences based on sampling season. Additionally, biodiversity (i.e., species richness, Shannon Diversity index) analyses were used to determine the macroinvertebrate and fish species richness and diversity of the three areas (DIVERSE; Primer-E version 7.0 software).

Environmental data collected during fish and macroinvertebrate sampling events were organized into two separate data sets. Both environmental data sets were missing values for water temperature at several sites, so the missing values were estimated prior to further analyses (Missing Routine, Primer-E version 7.0 software). Draftsman plots were generated from each environmental data set and were used to evaluate data symmetry and correlations among variables. No correlations were found among environmental measures for either data set (Spearman correlation <0.9), indicating no redundancy between variables. Thus, no environmental variables were removed from the representative data sets. The environmental variables within each data set were normalized to make them comparable between one another, and Euclidean Distance similarity matrices were constructed from the normalized data sets.

The fish and macroinvertebrate abundance and environmental ordinations of samples were compared using BIOENV analyses, resulting in combinations of environmental variables that are highly correlated with the ordination of community samples. In addition, principal components analyses (PCA, Primer-E version 7.0 software) were performed to visualize the variation among fish and macroinvertebrate samples based on their respective environmental variables. Next, model matrices were created from the latitude and longitude of fish and macroinvertebrate samples, and RELATE analyses were performed to examine the relationship

between fish and macroinvertebrate abundance and geographic position, which compares the ranked similarities of the species abundance resemblance matrices to those of the model matrices. If the relationships between samples agree entirely between the sample and model resemblance matrices, then the rank correlation is equal to 1. In addition, one-way similarity percentage analyses were performed from the standardized (fish) and transformed (macroinvertebrate) abundance data matrices to quantify the contribution of each species to the similarity and dissimilarity among the three areas (i.e., BG-S, BG-NW, BG-NE; SIMPER, Primer-E version 7.0 software).

To further visualize any differences in community composition between the three areas, fish species abundances were summed for each area and macroinvertebrates were categorized into three distinct taxonomical groups: 1) Polychaeta, 2) Molluska, and 3) Crustacea. The resulting numbers were then plotted on pie graphs to visualize differences in fish and macroinvertebrate communities between BG-S, BG-NE, and BG-NW. A pie graph of fish species abundances for the entire Bahia Grande was also created to visualize the contribution of dominant species to overall fish community structure. Lastly, dominance curves, in which species are ranked by their relative abundances and the percentage of the number of individuals of each species is plotted against the log species rank, were created for both fish and macroinvertebrate communities in order to visualize the dominance among the three areas (Dominance Plot, Primer-E version 7.0 software).

To test for differences in fish and macroinvertebrate community structure based on seagrass coverage, a shapefile containing x,y data (i.e., geographic location coordinates) of the 83 fish and 48 macroinvertebrate sampling sites were overlaid onto the seagrass classification map generated in ERDAS Imagine. Each sampling site was grouped into one of the three classes

representing seagrass coverage (i.e., dense, moderate, bare/sparse) based on its location on the classification map. Bray-Curtis similarity matrices were constructed from the fish and macroinvertebrate data sets, and a design matrix was formulated from the factor identifier for seagrass coverage (fixed factor). Groups (i.e., dense, moderate, bare/sparse) for both fish and macroinvertebrates were then compared using a PERMANOVA, which was selected because of the unequal number of samples within each seagrass classification group. Type III (partial) sum of squares and unrestricted permutation of raw data settings were selected, which are recommended for unbalanced one-way analyses. Next, mMDS analyses were performed from the two similarity matrices based upon 100 bootstrap averages from each group to visualize the similarities among fish and macroinvertebrate samples within groups. Additionally, one-way similarity percentage analyses (SIMPER, Primer-E version 7.0 software) were performed from the standardized (fish) and transformed (macroinvertebrate) data matrices to quantify the contribution of each species to the similarity and dissimilarity among the three seagrass coverage groups (i.e., dense, moderate, bare/sparse). Lastly, DIVERSE analyses were used to determine the macroinvertebrate and fish species richness and diversity of the three seagrass coverage groups.

Figure 3. Location of salinity sampling sites. Sites 1-34 are located in the south Bahia Grande and sites 35-71 are located in the north Bahia Grande.

Figure 4. Location of sampling sites for trace gas measurements. Locations selected based on salinity gradient map generated in ArcGIS (Figure 8). Sites S1-9 are located in the south Bahia Grande, while sites N1-9 are located in the north Bahia Grande.

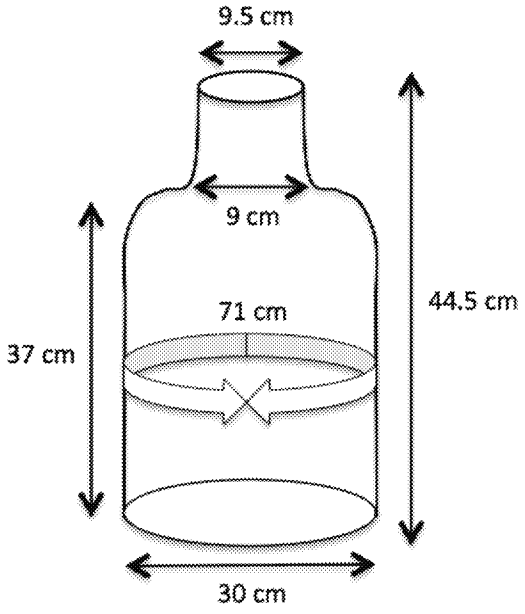

Figure 5. Diagram of the Chemglass benthic chamber used to collect gas flux measurements in the Bahia Grande.

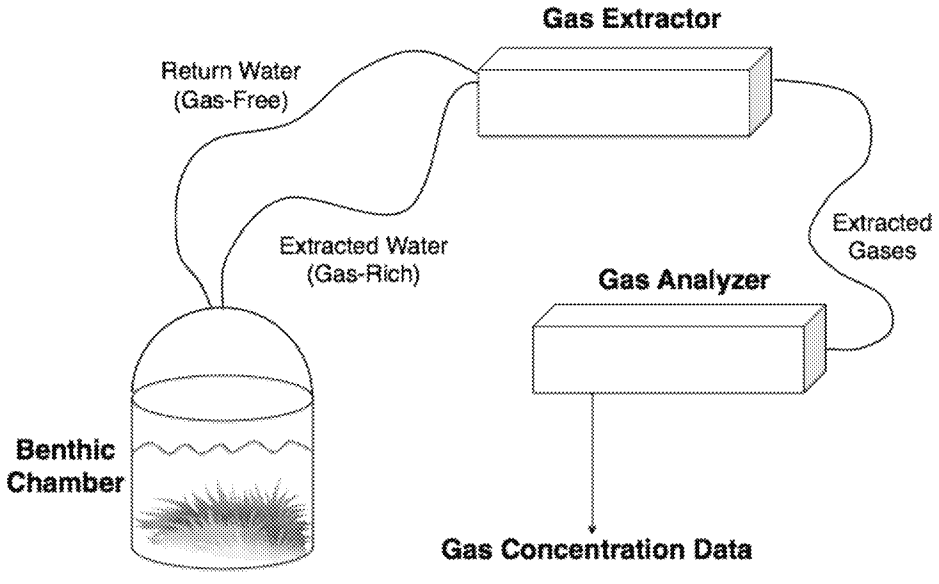

Figure 6. Schematic showing the process of gas extraction and analysis using Chemglass benthic chambers and Los Gatos Gas Extraction Unit and Analyzer.

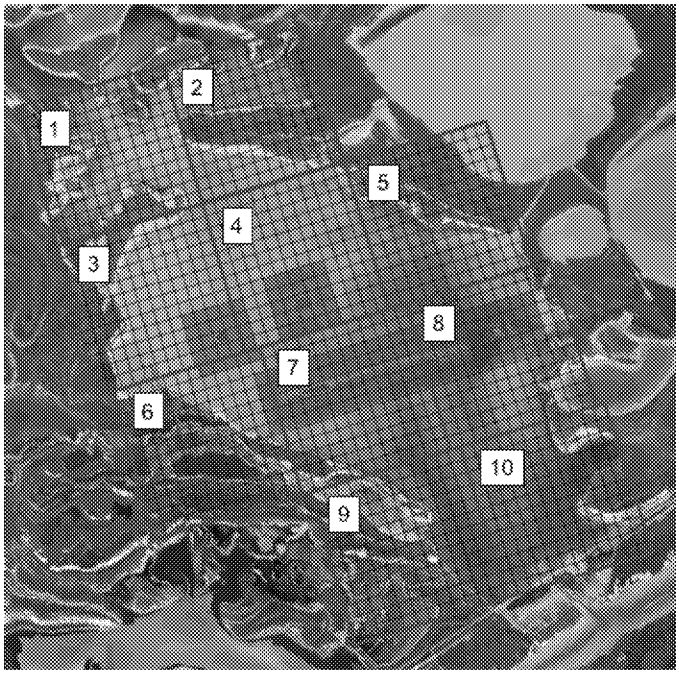

Figure 7. Map of Bahia Grande showing fish sampling grids and gridlets. Pink outlines indicate the 10 grids, while smaller black outlines indicate the 144 gridlets within each larger grid. Red areas were excluded from random sampling due to their proximity to bird habitats on the islands.

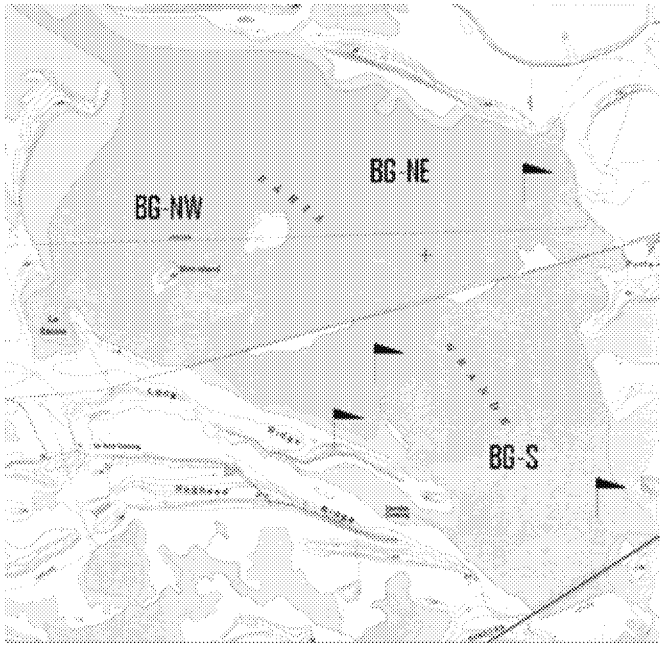

Figure 8. Map of Bahia Grande showing the three benthic sampling areas: Bahia Grande South (BG-S), Bahia Grande Northwest (BG-NW), and Bahia Grande Northeast (BG-NE). The pilot channel opens into BG-S. The line separating BG-S and BG-NW/BG-NE is the historic railroad trestle (Hicks et al. 2010). Black flags indicate former water quality monitoring stations.

CHAPTER III

RESULTS

Salinity Patterns

The salinity gradient map of the Bahia Grande revealed an increase in salinity in a northwest direction (Figure 9). Salinities were lowest (e.g., 36-45) in BG-S and highest (e.g., 91-178) in the northernmost areas of BG-NW. Based on the salinity data collected for gradient mapping (i.e., on a single event under typical conditions), the southern area of the basin (i.e., south of the railroad trestle) had an average salinity of 39.7, while the northern area of the basin (i.e., north of the railroad trestle) had an average salinity of 73.4. Further, the northeastern area had an average salinity of 67.5 while the northwestern area had an average salinity of 80.3. The temperature gradient map also showed an increase in water temperature in a northern direction, with average temperatures being the lowest in the southern area (29.2°C) and highest in the northwestern area (31.5°C; Figure 10)

Seagrass Distribution

The seagrass distribution map of the Bahia Grande revealed a decrease in seagrass coverage in a northwest direction (Figure 11). Seagrass coverage was higher in the southern area of the basin near the inlet channel and lower in northern areas farthest from the inlet channel. The majority of the basin had bare/sparse seagrass coverage (54.15%), while 27.66% of the basin was dense, and the remaining 18.19% was moderate. The only seagrass species observed in the

Bahia Grande in this project was *H. wrightii*.

Trace Gas Fluxes

A strong positive correlation between salinity and sulfate concentration (Spearman correlation >0.9) existed. The DISTLM analysis revealed that the best combination of predictor variables for CO_2 and CH_4 fluxes were water temperature and organic carbon content (AIC_c = -42.70, R^2 = 0.4). Two dbRDA axes accounted for 39.9% of the total variation among predictor variables (Figure 12). Axis one (dbRDA 1) accounted for 39.9% of the variation, while axis two (dbRDA 2) accounted for 0% of the variation. One of the selected predictor variables (i.e., carbon content) contributed more to dbRDA 1, while the other predictor variable (i.e., water temperature) contributed more to dbRDA 2. No difference in trace gas fluxes were observed based on area (i.e., south vs. north; R_{ANOSIM} = 0.05; p = 0.2), seagrass coverage (i.e., dense vs. moderate vs. bare/sparse; pseudo-F = 1.82, p = 0.19), or geographic position of samples (i.e., latitude and longitude; ρ = -0.03, p = 0.58). Trace gas fluxes also did not differ significantly based on time of day (pseudo-F = 0.489, p = 0.69) or sampling date (pseudo-F = 1.116, p = 0.30).

Percent organic carbon and nitrogen content of the sediment was not significantly different between southern and northern regions (R_{ANOSIM} = 0; p = 0.36). The nMDS supported these results, as there is no clear separation between southern and northern samples despite large differences in salinity between the two areas (Figure 13). In addition, carbon and nitrogen content did not differ based on the geographic position where samples were taken (i.e., latitude and longitude; ρ = -0.02, p = 0.53). The BIOENV routine revealed that the composition of organic carbon and nitrogen samples displayed the highest correlation with the combination of water temperature and seagrass coverage (ρ = 0.20). The PERMANOVA further revealed that

organic carbon and nitrogen content was significantly different based on seagrass coverage (pseudo-F = 3.918, p = 0.04; Table 1). There were significant differences between dense and bare/sparse (pseudo-F = 3.365, p < 0.01) and bare/sparse and moderate seagrass coverages (pseudo-F = 2.340, p = 0.03). There was not a significant difference in carbon and nitrogen content between dense and moderate seagrass coverages (pseudo-F = 0.604, p = 0.57). Plots of percent organic carbon and nitrogen at different depths (i.e., 0-2 cm, 2-4 cm) showed that values were higher at 0-2 cm than in 2-4 cm at most sites (Figure 14a-b). The maps showing percent organic carbon and nitrogen content in relation to seagrass coverage showed higher content in moderate and dense areas than bare/sparse areas (Figure 15a-b). It is important to note that although not visible on the map, the two southernmost sites are found within areas of bare/sparse seagrass coverage.

Fish Community Structure

Fish communities differed among the three areas sampled (pseudo-F = 3.766, $p = 0.003$; Table 2). Fish communities significantly differed between BG-S and BG-NW (pseudo-F = 2.523, $p < 0.001$) and BG-S and BG-NE (pseudo-F = 1.870, $p = 0.014$), but not between BG-NW and BG-NE (pseudo-F = 0.972, $p = 0.343$). The bootstrap-averaged mMDS (Figure 16) revealed a separation of samples between BG-S and both BG-NW and BG-NE, but no separation between BG-NW and BG-NE, supporting the results from the PERMANOVA analysis. DIVERSE analysis revealed that species richness and diversity were highest for BG-S (S = 20, H' = 1.70), followed by BG-NE (S = 12, H' = 1.07) and BG-NW (S =11, H' = 0.97). No differences in fish community structure were observed between sampling month (F = 1.192, $p = 0.286$) or geographic position where samples were taken (i.e., longitude and latitude; RELATE test, ρ = 0.079, p = 0.006).

The BIOENV routine revealed that the composition of fishes displayed the highest correlation with depth alone ($\rho = 0.411$) or depth and salinity ($\rho = 0.348$). Two PCA axes accounted for 76.4% of the variation among environmental variables. Principal component one (PC Axis 1) accounted for 41.0% of the variation, while principal component two (PC Axis 2) accounted for 35.4% of the variation. Three variables (i.e., depth, dissolved oxygen, and salinity) contributed most to PC Axis 1, whereas one variable (i.e., temperature) contributed more to PC Axis 2. Samples from BG-S were concentrated in areas of lower salinity and higher depth, while a distinct group of samples from BG-NE and BG-NW were concentrated in areas of higher salinity and lower depth (Figure 17). There was some overlap between northern samples that were located closer to the railroad trestle and southern samples, indicating more similarity between communities in these areas in relation to environmental variables.

The SIMPER analysis showed that the average similarity among samples within BG-S, BG-NE, and BG-NW samples were due primarily to one species, *C. variegatus* (76.13%, 96.30%, and 97.92%, respectively; Table 3a-c). Differences between BG-S and BG-NE, and BG-NW and BG-NE were due primarily to the higher contribution of *C. variegatus* to fish communities in BG-NE than in BG-S or BG-NW (Table 3d,f). Similarly, differences between BG-S and BG-NW were related primarily to the higher contribution of *C. variegatus* to BG-S than BG-NW (Table 3e).

Pie graphs of species compositions further highlighted the variations in fish communities between the three areas (Figure 18). *C. variegatus* dominated fish communities in all three areas, but in varying degrees (i.e., BG-S (48%), BG-NW (72%), BG-NE (78%)). Seven species comprised over 96% of all fish in BG-S, while only four species comprised over 96% of all fish in both BG-NE and BG-NW. Within the entire Bahia Grande, *C. variegatus* comprised 58% of

all fish and eight species comprised 96% of all fish (Figure 19). A dominance curve indicated high dominance by a single species (*C. variegatus*) in each of the three sampling areas: northeastern (~78%), northwestern (~72%), and southern (~48%) areas (Figure 20).

Fish communities were significantly different based on seagrass coverage (pseudo-F = 10.593, $p < 0.001$; Table 4). Communities within areas of dense seagrass coverage were significantly different from those in both moderate (pseudo-F = 3.773, $p < 0.001$) and bare/sparse seagrass coverages (pseudo-F = 2.921, $p < 0.001$). Communities were also different between areas of moderate and bare/sparse seagrass coverage (pseudo-F = 3.233, $p < 0.001$). The mMDS based on bootstrap averages revealed a separation of samples between all three groups, supporting the results from the PERMANOVA analysis (Figure 21).

The SIMPER revealed that the average similarity of samples within the dense seagrass coverage category was due primarily to *Pogonias cromis* (62.39%) and *Ariopsis felis* (26.43%; Table 5a). Average similarity of samples within both moderate and bare/sparse categories was due almost entirely to one species, *C. variegatus* (89.38% and 98.46%, respectively; Table 5b-c). Differences between moderate and bare/sparse samples were primarily due to the higher abundance of *C. variegatus* within the fish communities in moderate than in bare/sparse seagrass areas (Table 5f). Differences between dense and bare/sparse, and dense and moderate samples were related to (1) dense areafish species *P. cromis* (37.29% and 26.91%, respectively) and *A. felis* (16.34% and 12.50%, respectively), and (2) bare/sparse and moderate area species *C. variegatus* (24.32% and 35.49%, respectively; Table 5d-e). DIVERSE analysis showed that species diversity was highest for moderate (H' = 1.403), followed by dense (H' = 1.371), and lowest for bare/sparse (H' = 0.990). Species richness was highest for moderate (S = 19), followed by bare/sparse (S = 14) and dense (S = 8).

Macroinvertebrate Community Structure

Macroinvertebrate communities were significantly different between BG-S and BG-NW (R_{ANOSIM} = 0.607; p = 0.01) and BG-S and BG-NE (R_{ANOSIM} = 0.381; p = 0.01), but not significantly different between BG-NW and BG-NE (R_{ANOSIM} = 0.133; p = 0.9). The nMDS (Figure 22) revealed two separate clusters (i.e., BG-S and BG-NW), with samples from BG-NE more similar to BG-NW, supporting the results from the ANOSIM analysis. DIVERSE analysis revealed that species richness and diversity were highest for BG-S (S = 21, H' = 2.158), followed by BG-NE (S = 16, H' = 0.9409), and lowest for BG-NW (S =10, H' = 0.8581). No differences in macroinvertebrate community structure were observed between sampling month (R_{ANOSIM} = 0.02, p = 0.175). The benthic macroinvertebrate community was significantly correlated with the geographic location of sample collection (i.e., longitude and latitude; RELATE test, ρ = 0.537, p < 0.001).

The BIOENV routine showed that the composition of macroinvertebrate fauna displayed the highest correlation with depth and salinity (ρ= 0.489). Two PCA axes accounted for 85.6% of the variation among environmental variables. Principal component one (PC Axis 1) accounted for 55.3% of the variation, while principal component two (PC Axis 2) accounted for 30.3% of the variation. Two variables (i.e., salinity and water temperature) contributed more to PC Axis 1, whereas one variable (i.e., depth) contributed more to PC Axis 2. Samples from BG-S were concentrated in areas of lower salinity, lower water temperature, and higher depth, while samples from BG-NW were concentrated in areas of higher salinity, higher water temperature, and lower depth (Figure 23). Overlap between northeastern and northwestern samples existed, indicating more similarity between communities in these areas in relation to environmental variables.

The SIMPER analysis showed that the similarity within BG-S samples was primarily due to polychaete family Capitellidae (44.95%; Table 6a). Average similarity within BG-NW and BG-NE were related to macroinvertebrate species *Anomalocardia auberiana* (60.95% and 64.49%, respectively) and *Mulinia lateralis* (25.99% and 19.68%, respectively; Table 6b-c). Differences between BG-S and BG-NW, and BG-NE and BG-NW were related primarily to the higher contribution of molluscan species *A. auberiana* and *M. lateralis* to communities in BG-NW than BG-S or BG-NE (Table 6e-f). Differences between BG-S and BG-NE were due to the higher contribution of *A. auberiana* and *M. lateralis* to BG-NE and higher contribution of Capitellidae to BG-S (Table 6d).

Grouping organisms based on taxonomical differences further highlighted the variations in benthic macroinvertebrate communities between the three areas (Figure 24). Polychaeta (50%) dominated macroinvertebrate communities in BG-S, followed by Mollusca (42%) and Crustacea (8%). In BG-NE, Mollusca (92%) dominated the community, followed by Crustacea (5%) and Polychaeta (3%). Mollusca (94%) dominated the macroinvertebrate community in BG-NW, with Crustacea (6%) comprising the remainder. A dominance curve indicated high dominance by a single species in each of the three sampling areas: northeastern (~78%), northwestern (~75%), and southern (~48%) areas (Figure 20). In northern areas, *A. auberiana* was the most dominant species, while polychaete family Capitellidae was the most dominant in southern areas.

Macroinvertebrate communities were significantly different based on seagrass coverage (pseudo-F = 7.955, $p < 0.001$; Table 7). Communities within areas of dense seagrass coverage were significantly different from those in both moderate (pseudo-F = 2.061, $p = 0.001$) and bare/sparse seagrass coverages (pseudo-F = 3.673, $p < 0.001$). Communities were also different

between areas of moderate and bare/sparse seagrass coverage (pseudo-F = 1.603, $p = 0.039$). The mMDS based on bootstrap averages revealed a separation of samples between all three groups, supporting the results from the PERMANOVA analysis (Figure 26).

The SIMPER analysis revealed that the similarity within bare/sparse and moderate samples was related primarily to *A. auberiana* (63.09% and 68.86%, respectively) and *M. lateralis* (27.44% and 12.67%, respectively; Table 8b-c). The average similarity within the dense seagrass group was due primarily to polychaete family Capitellidae (31.20%; Table 8a). Differences between all groups were largely due to differences in the contribution of *A. auberiana* and *M. lateralis* to macroinvertebrate communities in the three seagrass groups (Table 8d-f). These two mollusks contributed most heavily to bare/sparse, followed by moderate and lastly dense seagrass beds. DIVERSE analysis showed that species richness and diversity were highest for dense (S = 22, H' = 2.266), followed by moderate (S = 12, H' = 1.038), and lowest for bare/sparse (S =12, H' = 0.736).

Table 1. One-way PERMANOVA analysis for percent organic carbon and nitrogen content of the sediment with seagrass coverage category as a fixed factor including degrees of freedom (df), sum of squares (SS), mean squares (MS), and number of unique permutations (perms).

Source	df	SS	MS	Pseudo-F	P (perm)	perms
Coverage	2	11.666	5.8331	3.9177	0.0402	9958
Residual	15	22.334	1.4889			
Total	17	34				

Table 2. One-way PERMANOVA analysis for fish community structure with sampling area as a fixed factor including degrees of freedom (df), sum of squares (SS), mean squares (MS), and number of unique permutations (perms).

Source	df	SS	MS	Pseudo-F	P (perm)	perms
Area	2	19857	9928.5	3.7662	0.0025	9932
Residual	80	2.109E+05	2636.2			
Total	82	2.308E+05				

Table 3 (a-f). One-way analysis of similarity (SIMPER) with a 70% cut off for low contributing species to fish community structure based on area including average abundance (Av.Abund), average similarity (Av.Sim), similarity standard deviation (Sim/SD), percent contribution (Contrib %), cumulative contribution (Cum %), average dissimilarity (Av.Diss), and dissimilarity standard deviation (Diss/SD).

(a)

Bahia Grande South (BG-S)

Average similarity: 39.03

Species	Av.Abund	Av.Sim	Sim/SD	Contrib %	Cum %
C. variegatus	52.31	29.71	0.89	76.13	76.13

(b)

Bahia Grande Northeast (BG-NE)

Average similarity: 36.18

Species	Av.Abund	Av.Sim	Sim/SD	Contrib %	Cum %
C. variegatus	57.77	34.84	0.89	96.30	96.30

(c)

Bahia Grande Northwest (BG-NW)

Average similarity: 39.03

Species	Av.Abund	Av.Sim	Sim/SD	Contrib %	Cum %
C. variegatus	49.77	27.43	0.68	97.92	97.92

(d)

Bahia Grande Northeast (BG-NE) vs. Bahia Grande South (BG-S)

Average dissimilarity: 65.86

Species	BG-NE Av.Abund	BG-S Av.Abund	Av.Diss	Diss/SD	Contrib%	Cum%
C. variegatus	57.77	52.31	28.37	1.07	43.07	43.07
P. cromis	1.32	18.07	11.15	0.61	16.92	59.99
M. cephalus	8.23	1.61	4.75	0.52	7.22	67.21
L. rhomboides	0.16	7.19	4.36	0.58	6.62	73.83

(e)

Bahia Grande Northwest (BG-NW) vs. Bahia Grande South (BG-S)

Average dissimilarity: 70.77

Species	BG-NW Av.Abund	BG-S Av.Abund	Av.Diss	Diss/SD	Contrib%	Cum%
C. variegatus	49.77	52.31	32.95	1.08	46.56	46.56
P. cromis	5.78	18.07	13.76	0.65	19.45	66.00
L. rhomboides	0.18	7.19	4.84	0.58	6.84	72.84

(f)
Bahia Grande Northwest (BG-NW) vs. Bahia Grande Northeast (BG-NE)
Average dissimilarity: 67.47

Species	BG-NW Av.Abund	BG-NE Av.Abund	Av.Diss	Diss/SD	Contrib%	Cum%
C. variegatus	49.77	57.77	42.51	1.10	63.01	63.01
M. cephalus	1.37	8.23	6.59	0.47	9.77	72.78

Table 4. One-way PERMANOVA analysis for fish community structure with seagrass coverage category as a fixed factor including degrees of freedom (df), sum of squares (SS), mean squares (MS), and number of unique permutations (perms).

Source	df	SS	MS	Pseudo-F	P (perm)	perms
Coverage	2	48315	24158	10.593	0.0001	9947
Residual	80	1.824E+05	2280.5			
Total	82	2.308E+05				

Table 5 (a-f). One-way SIMPER with a 70% cut off for low contributing species to fish community structure based on seagrass coverage category including average abundance (Av.Abund), average similarity (Av.Sim), similarity standard deviation (Sim/SD), percent contribution (Contrib %), cumulative contribution (Cum %), average dissimilarity (Av.Diss), and dissimilarity standard deviation (Diss/SD).

(a)

Dense

Average similarity: 50.35

Species	Av.Abund	Av.Sim	Sim/SD	Contrib %	Cum %
P. cromis	53.15	31.42	1.05	62.39	62.39
A. felis	23.03	13.31	0.95	26.43	88.82

(b)

Moderate

Average similarity: 50.05

Species	Av.Abund	Av.Sim	Sim/SD	Contrib %	Cum %
C. variegatus	64.56	44.73	1.31	89.38	89.38

(c)

Bare/sparse

Average similarity: 26.25

Species	Av.Abund	Av.Sim	Sim/SD	Contrib %	Cum %
C. variegatus	47.34	25.84	0.66	98.46	98.46

(d)
Moderate vs. Dense
Average dissimilarity: 90.94

Species	Moderate Av.Abund	Dense Av.Abund	Av.Diss	Diss/SD	Contrib%	Cum%
C. variegatus	64.56	0.10	32.28	1.84	35.49	35.49
P. cromis	10.13	53.15	24.47	1.57	26.91	62.40
A. felis	0.58	23.03	11.37	1.59	12.50	74.91

(e)
Bare/sparse vs. Dense
Average dissimilarity: 70.77

Species	Bare/sparse Av.Abund	Dense Av.Abund	Av.Diss	Diss/SD	Contrib%	Cum%
P. cromis	3.26	53.15	36.29	1.35	37.29	37.29
C. variegatus	47.34	0.10	23.67	1.02	24.32	61.60
A. felis	0.10	23.03	15.91	1.32	16.34	77.95

(f)

Bare/sparse vs. Moderate

Average dissimilarity: 67.03

Species	Bare/sparse Av.Abund	Moderate Av.Abund	Av.Diss	Diss/SD	Contrib%	Cum%
C. variegatus	47.34	64.56	36.66	1.09	54.68	54.68
P. cromis	3.26	10.13	8.18	0.47	12.21	66.89
Menidia sp.	1.58	5.67	4.32	0.57	6.44	73.33

Table 6 (a-f). One-way SIMPER with a 70% cut off for low contributing species to macroinvertebrate community structure based on area including average abundance (Av.Abund), average similarity (Av.Sim), similarity standard deviation (Sim/SD), percent contribution (Contrib %), cumulative contribution (Cum %), average dissimilarity (Av.Diss), and dissimilarity standard deviation (Diss/SD).

(a)

Bahia Grande South (BG-S)

Average similarity: 25.34

Species	Av.Abund	Av.Sim	Sim/SD	Contrib %	Cum %
Capitellidae	1.77	11.39	0.83	44.95	44.95
Cerithiidae	0.82	3.37	0.44	13.28	58.23
Spionidae	0.64	2.97	0.52	11.72	69.96
Nemertea	0.51	1.96	0.36	7.73	77.69

(b)
Bahia Grande Northeast (BG-NE)
Average similarity: 40.58

Species	Av.Abund	Av.Sim	Sim/SD	Contrib %	Cum %
A. auberiana	4.05	26.17	1.99	64.49	64.49
M. lateralis	1.43	7.99	0.83	19.68	84.18

(c)
Bahia Grande Northwest (BG-NW)
Average similarity: 62.74

Species	Av.Abund	Av.Sim	Sim/SD	Contrib %	Cum %
A. auberiana	5.46	38.24	3.04	60.95	60.95
M. lateralis	2.51	16.31	1.82	25.99	86.94

(d)

Bahia Grande South (BG-S) vs. Bahia Grande Northeast (BG-NE)

Average dissimilarity: 79.96

Species	BG-NE Av.Abund	BG-S Av.Abund	Av.Diss	Diss/SD	Contrib%	Cum%
A. auberiana	0.74	4.05	22.33	1.34	27.92	27.92
Capitellidae	1.77	0.51	10.85	1.12	13.57	41.49
M. lateralis	0.65	1.43	8.98	1.09	11.24	52.72
Cerithidae	0.82	0.28	6.24	0.66	7.81	60.53
Aoridae	0.35	0.61	4.51	0.88	5.64	66.17
A. papyrium	0.46	0.28	3.42	0.69	6.47	70.70

(e)

Bahia Grande Northwest (BG-NW) vs. Bahia Grande South (BG-S)

Average dissimilarity: 70.77

Species	BG-NW Av.Abund	BG-S Av.Abund	Av.Diss	Diss/SD	Contrib%	Cum%
A. auberiana	49.77	52.31	32.95	1.08	46.56	46.56
M. lateralis	5.78	18.07	13.76	0.65	19.45	66.00
Capitellidae	0.18	7.19	4.84	0.58	6.84	72.84
Aoridae	1.17	0.35	6.41	1.24	7.81	68.70
Cerithiidae	0.46	0.82	5.97	0.73	7.27	75.97

(f)
Bahia Grande Northwest (BG-NW) vs. Bahia Grande Northeast (BG-NE)
Average dissimilarity: 67.47

Species	BG-NW Av.Abund	BG-NE Av.Abund	Av.Diss	Diss/SD	Contrib%	Cum%
A. auberiana	5.46	4.05	19.19	1.65	36.34	36.34
M. lateralis	2.51	1.43	9.30	1.29	17.62	53.96
Aoridae	1.17	0.61	5.42	1.13	10.26	64.22
Cerithiidae	0.46	0.28	3.42	0.69	6.47	70.70

Table 7. One-way PERMANOVA analysis for macroinvertebrate community structure with the seagrass coverage category as a fixed factor including degrees of freedom (df), sum of squares (SS), mean squares (MS), and number of unique permutations (perms).

Source	df	SS	MS	Pseudo-F	P (perm)	perms
Coverage	2	24050	12025	7.9551	0.0001	9929
Residual	45	68022	1511.6			
Total	47	92073				

Table 8 (a-f). One-way SIMPER with a 70% cut off for low contributing species to macroinvertebrate community structure based on seagrass coverage category including average abundance (Av.Abund), average similarity (Av.Sim), similarity standard deviation (Sim/SD), percent contribution (Contrib %), cumulative contribution (Cum %), average dissimilarity (Av.Diss), and dissimilarity standard deviation (Diss/SD).

(a)

Dense

Average similarity: 24.40

Species	Av.Abund	Av.Sim	Sim/SD	Contrib %	Cum %
Capitellidae	1.42	7.61	0.65	31.20	31.20
A. auberiana	1.01	4.55	0.51	18.63	49.83
M. lateralis	0.79	3.04	0.47	12.47	62.31
Cerithiidae	0.69	2.99	0.41	12.25	74.56

(b)

Moderate

Average similarity: 47.21

Species	Av.Abund	Av.Sim	Sim/SD	Contrib %	Cum %
A. auberiana	4.34	32.51	2.68	68.86	68.86
M. lateralis	1.67	5.98	0.62	12.67	81.53

(c)
Bare/sparse
Average similarity: 60.23

Species	Av.Abund	Av.Sim	Sim/SD	Contrib %	Cum %
A. auberiana	5.95	38.00	3.11	63.09	63.09
M. lateralis	2.37	16.53	1.99	27.44	90.54

(d)
Dense vs. Moderate
Average dissimilarity: 75.08

Species	Dense Av.Abund	Moderate Av.Abund	Av.Diss	Diss/SD	Contrib%	Cum%
A. auberiana	1.01	4.34	22.47	1.62	29.93	29.93
M. lateralis	0.79	1.67	10.28	1.11	13.69	43.62
Capitellidae	1.42	0.48	8.92	1.00	11.89	55.50
A. papyrium	0.39	0.87	5.58	0.99	7.44	62.94
Aoridae	0.44	0.78	5.15	1.09	6.86	69.80
Cerithiidae	0.69	0.13	4.93	0.60	6.57	76.37

(e)
Bare/sparse vs. Dense
Average dissimilarity: 76.62

Species	Bare/sparse Av.Abund	Dense Av.Abund	Av.Diss	Diss/SD	Contrib%	Cum%
A. auberiana	5.95	1.01	28.01	1.89	36.55	36.55
M. lateralis	2.37	0.79	10.95	1.40	14.30	50.85
Capitellidae	0.08	1.42	7.82	0.97	10.21	61.06
Aoridae	1.00	0.44	5.62	1.06	7.33	68.39

(f)
Bare/sparse vs. Moderate
Average dissimilarity: 48.38

Species	Bare/sparse Av.Abund	Moderate Av.Abund	Av.Diss	Diss/SD	Contrib%	Cum%
A. auberiana	5.95	4.34	16.36	1.38	33.83	33.83
M. lateralis	2.37	1.67	9.88	1.55	20.42	54.25
Aoridae	1.00	0.78	4.85	1.13	10.02	64.27
A. papyrium	0.06	0.87	4.45	1.05	9.19	73.46

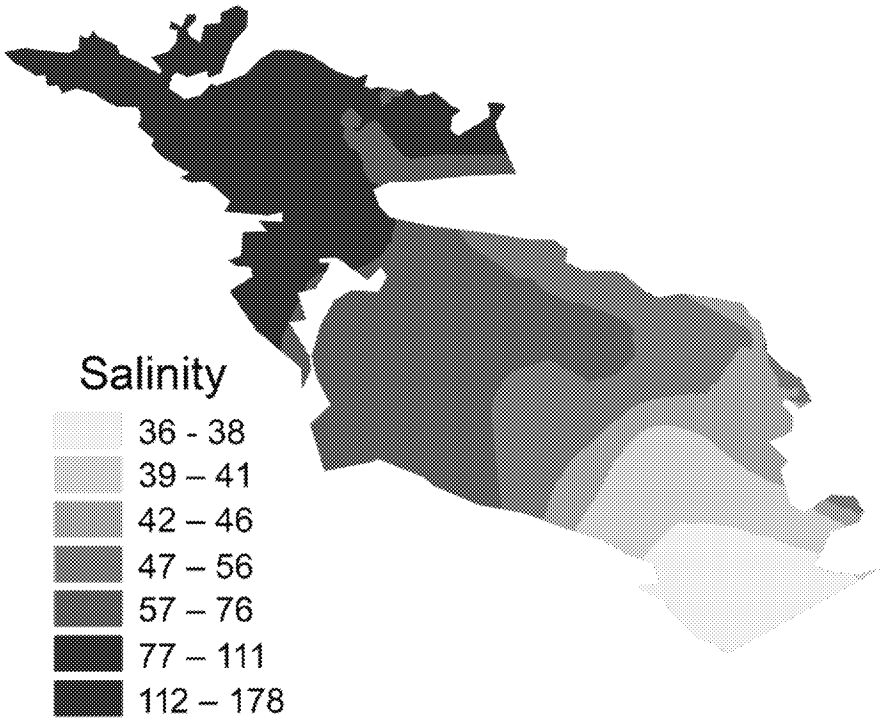

Figure 9. Salinity gradient map for the Bahia Grande based on salinity values at 71 sites.

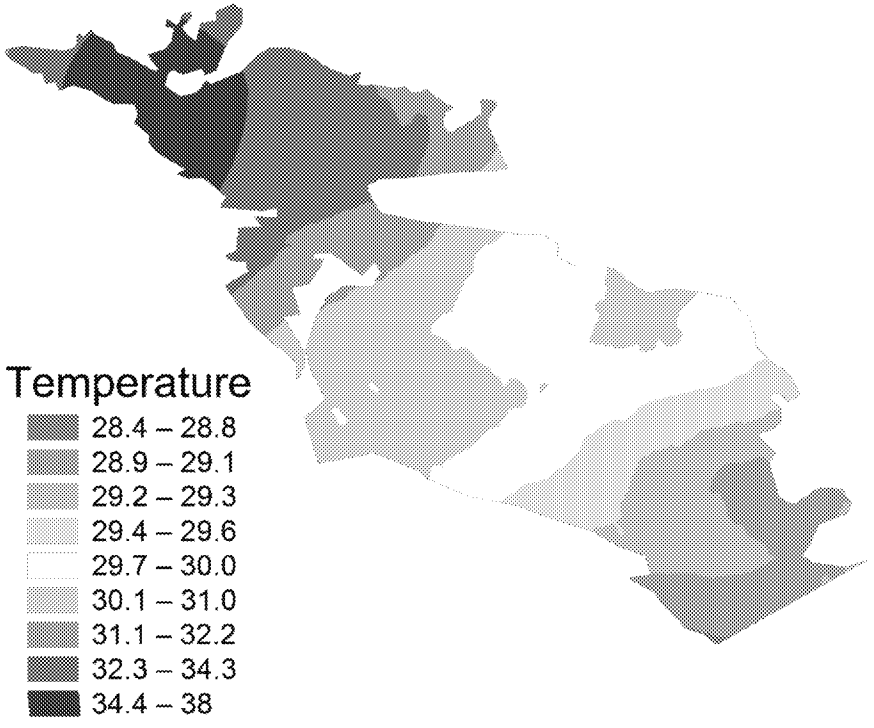

Figure 10. Water temperature gradient map for the Bahia Grande based on temperature values at 71 sites.

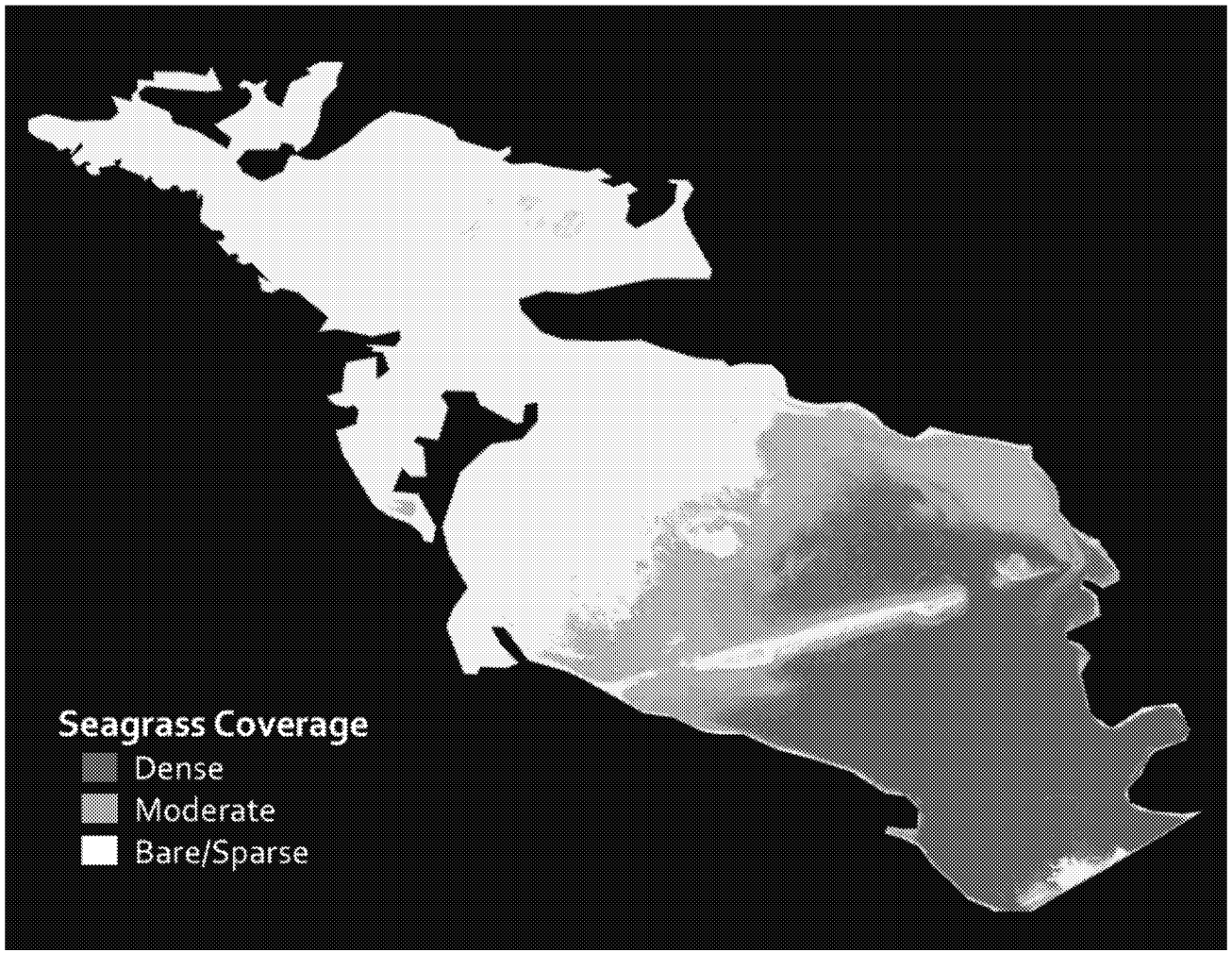

Figure 11. Seagrass distribution map for the Bahia Grande based on a supervised classification using 71 ground truth points.

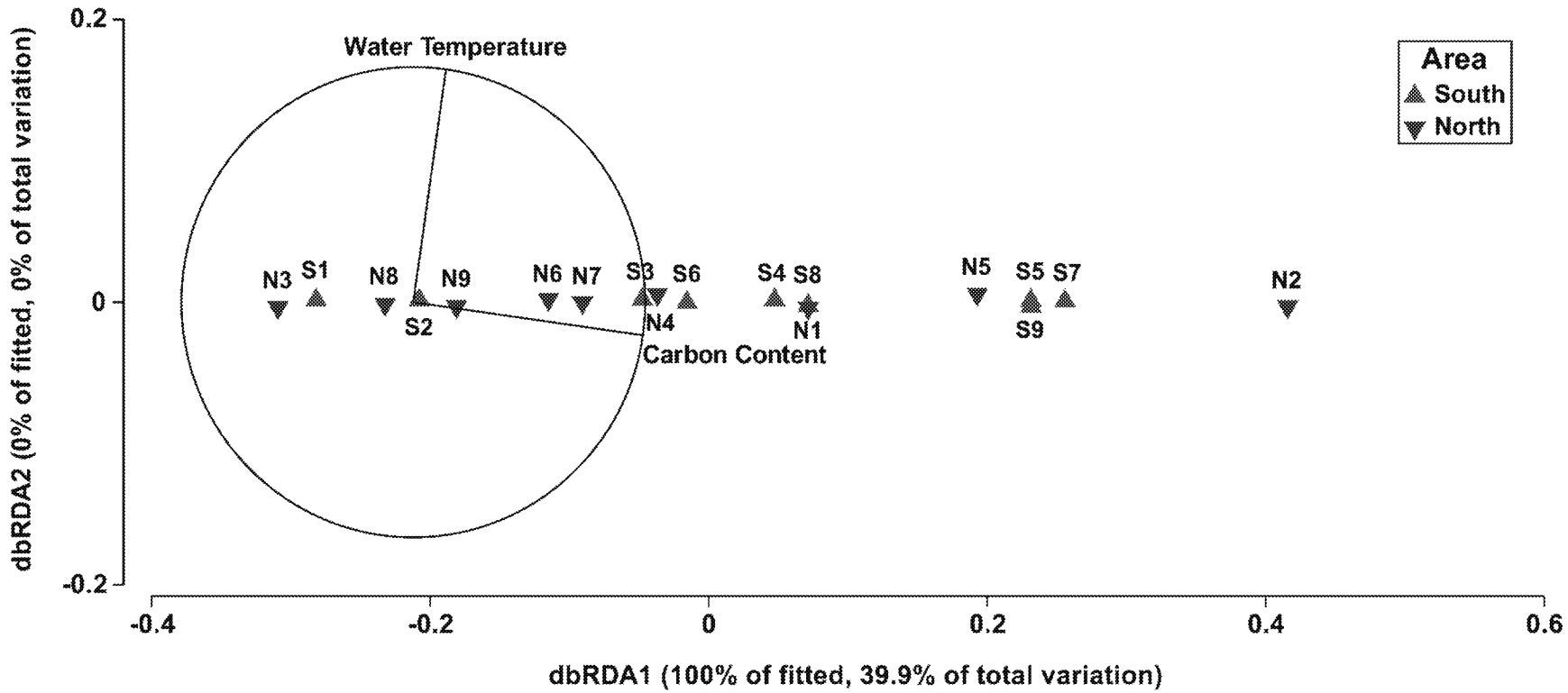

Figure 12. dbRDA plot of selected predictor variables (i.e., water temperature, % organic carbon content of the sediment) in relation to CO_2 and CH_4 fluxes in the Bahia Grande, Texas at nine southern and nine northern sites. Black lines indicate the direction in which the associated variable increases.

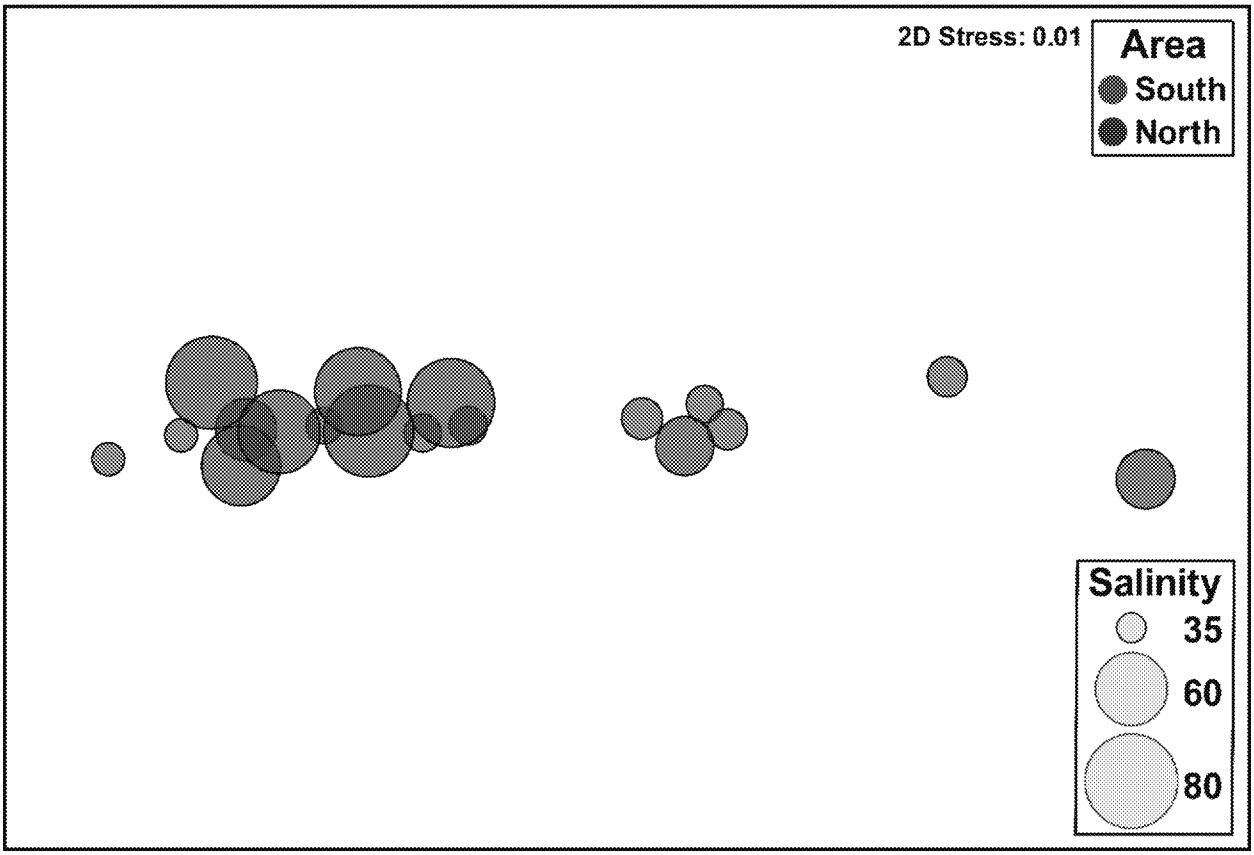

Figure 13. nMDS based on Euclidian distance similarities among percent organic carbon and total nitrogen content of the sediment samples collected at nine southern and nine northern sites in the Bahia Grande. Two-dimensional bubbles show the relationship between salinity and carbon and nitrogen content at various sites.

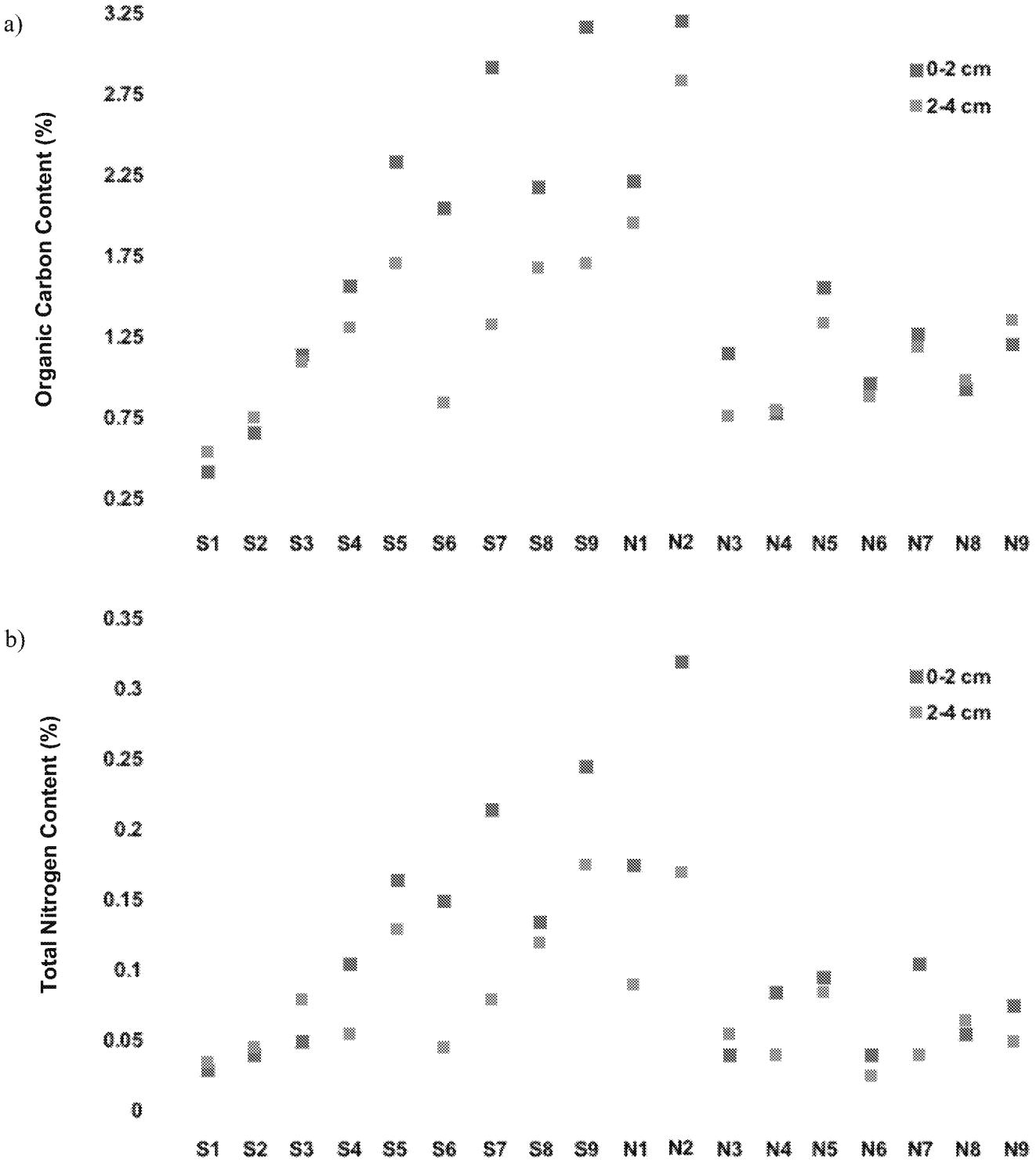

Figure 14 (a-b). Graphs showing the sediment organic carbon (a) and total nitrogen (b) content (%) at 0-2 cm and 2-4 cm at 18 sites along a salinity gradient line in the reflooded Bahia Grande. S1 is the southernmost site, while N9 is the northernmost site.

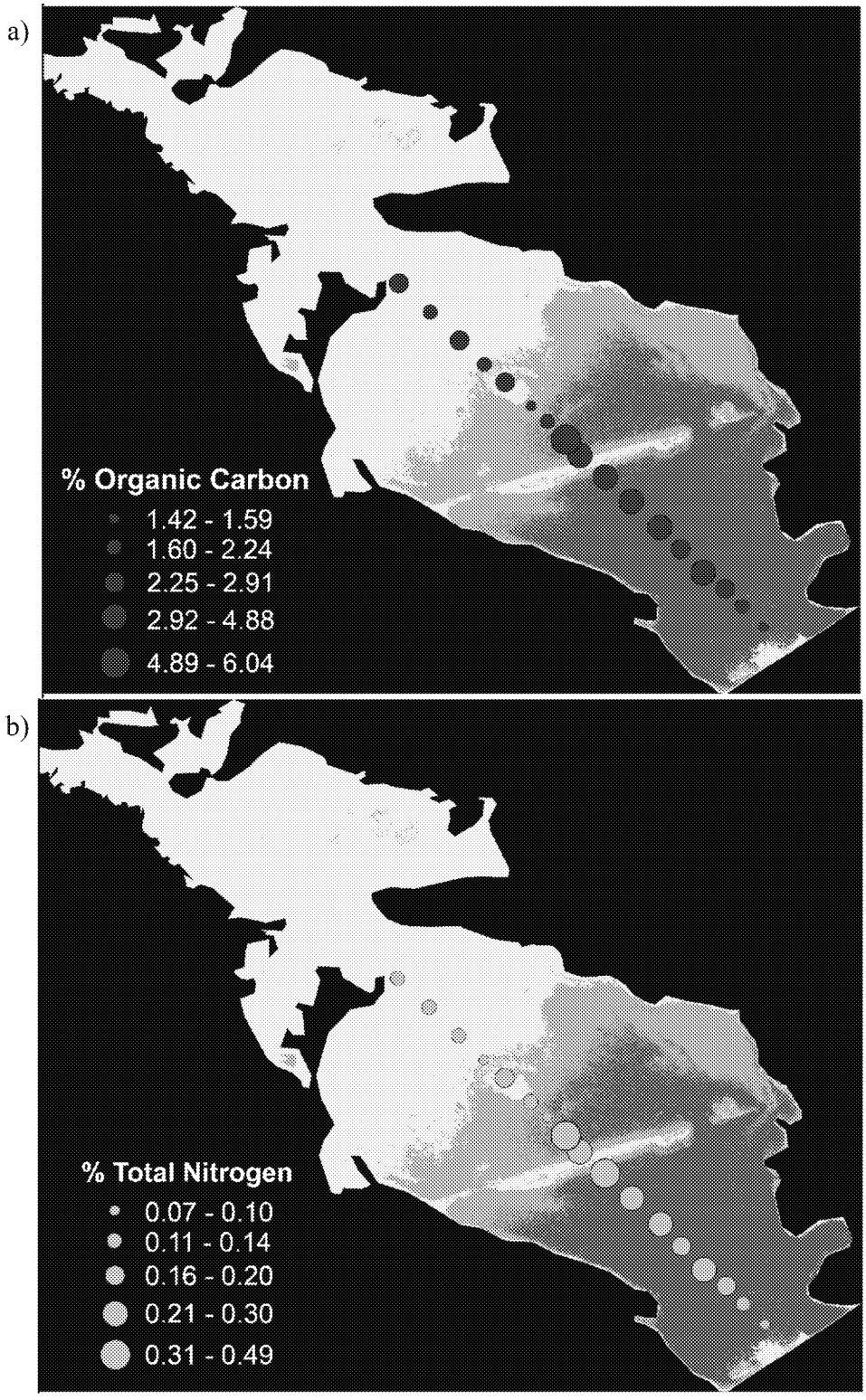

Figure 15 (a-b). Maps showing the percent organic carbon (a) and total nitrogen (b) content of the sediment in relation to seagrass coverage at 18 sites in the Bahia Grande. Dark blue areas on the underlying map represent areas of dense seagrass coverage, while light blue represent moderate, and white represent bare/sparse.

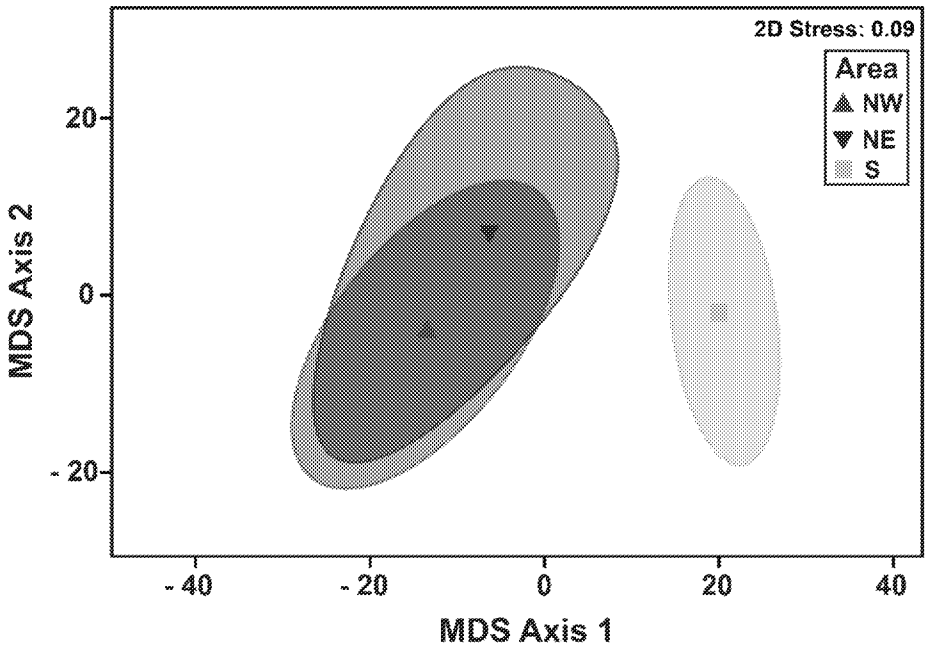

Figure 16. mMDS based on 100 bootstrap averages of fish community samples in three areas of the Bahia Grande (i.e., BG-S, BG-NW, and BG-NE).

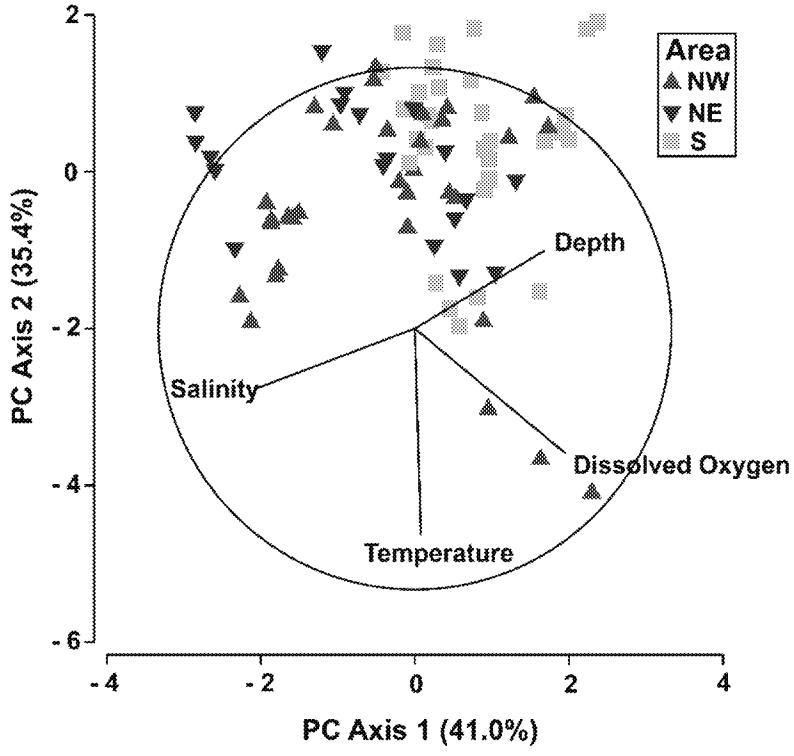

Figure 17. PCA plot of environmental variables (i.e., salinity, depth, temperature, dissolved oxygen) in the Bahia Grande at 83 fish sampling sites during three sampling events. Black lines indicate the direction in which the associated variable increases.

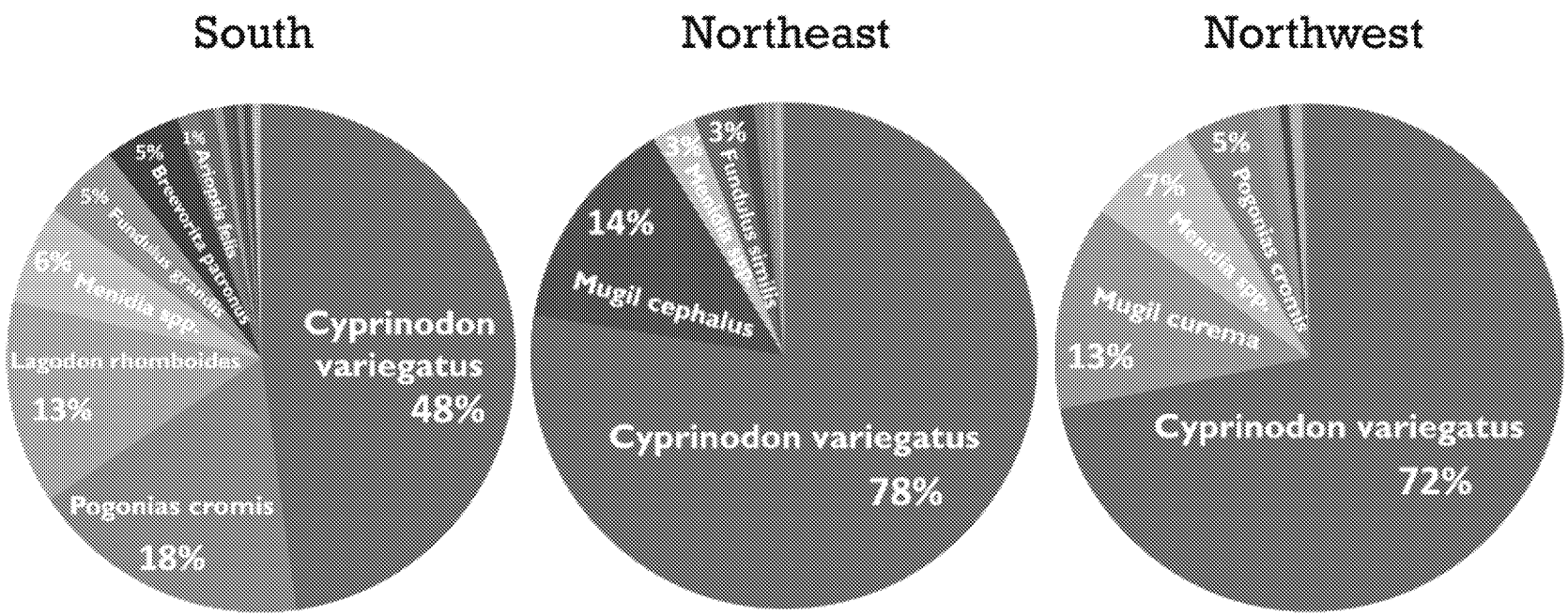

Figure 18. Pie graphs showing the composition of fish communities in three areas of the Bahia Grande (i.e., BG-S, BG-NW, BG-NE). The names of the species contributing most to the community structure of each area are listed in white.

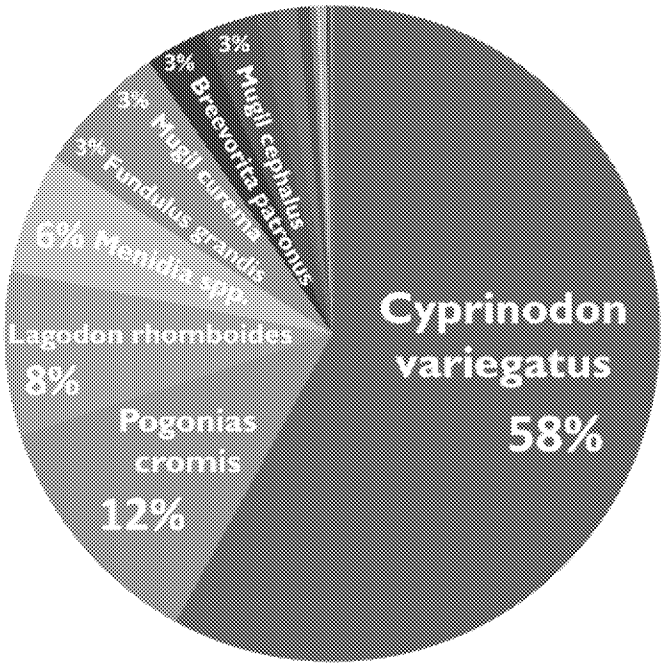

Figure 19. Pie graph showing the composition of fish communities in the Bahia Grande. The names of the species contributing most to the community are listed in white.

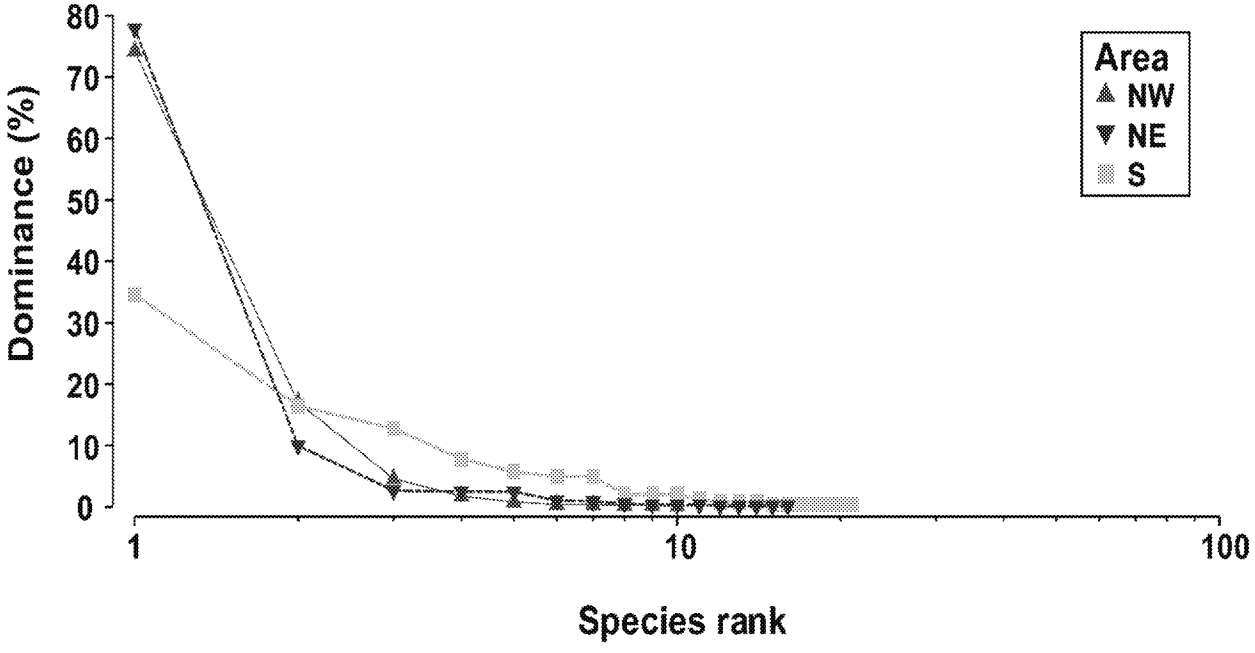

Figure 20. Dominance curve depicting the percentage of the fish community dominated by individual species in each area (i.e., BG-S, BG-NE, and BG-NW). Samples were collected at 83 individual sites in the Bahia Grande.

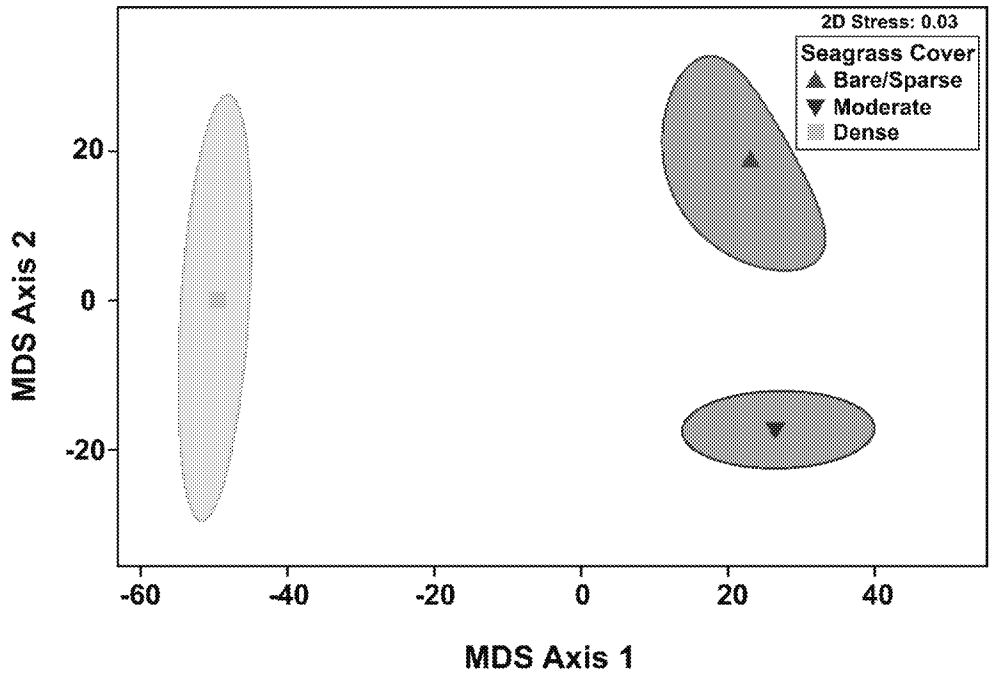

Figure 21. mMDS based on 100 bootstrap averages of fish species abundances in the Bahia Grande at 83 sampling sites grouped by seagrass coverage category (i.e., dense, moderate, bare/sparse).

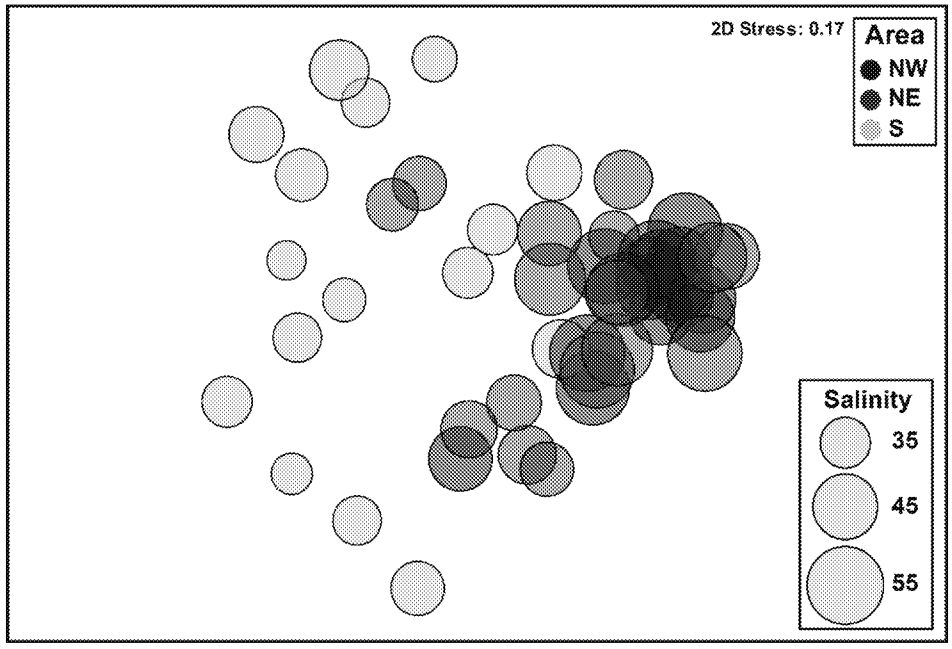

Figure 22. nMDS based on Bray-Curtis similarities among benthic macroinvertebrate abundances collected at sites in three areas of the Bahia Grande (i.e., BG-S, BG-NW, and BG-NE). Two-dimensional bubbles show the relationship between salinity and benthic macroinvertebrate abundance at various sites.

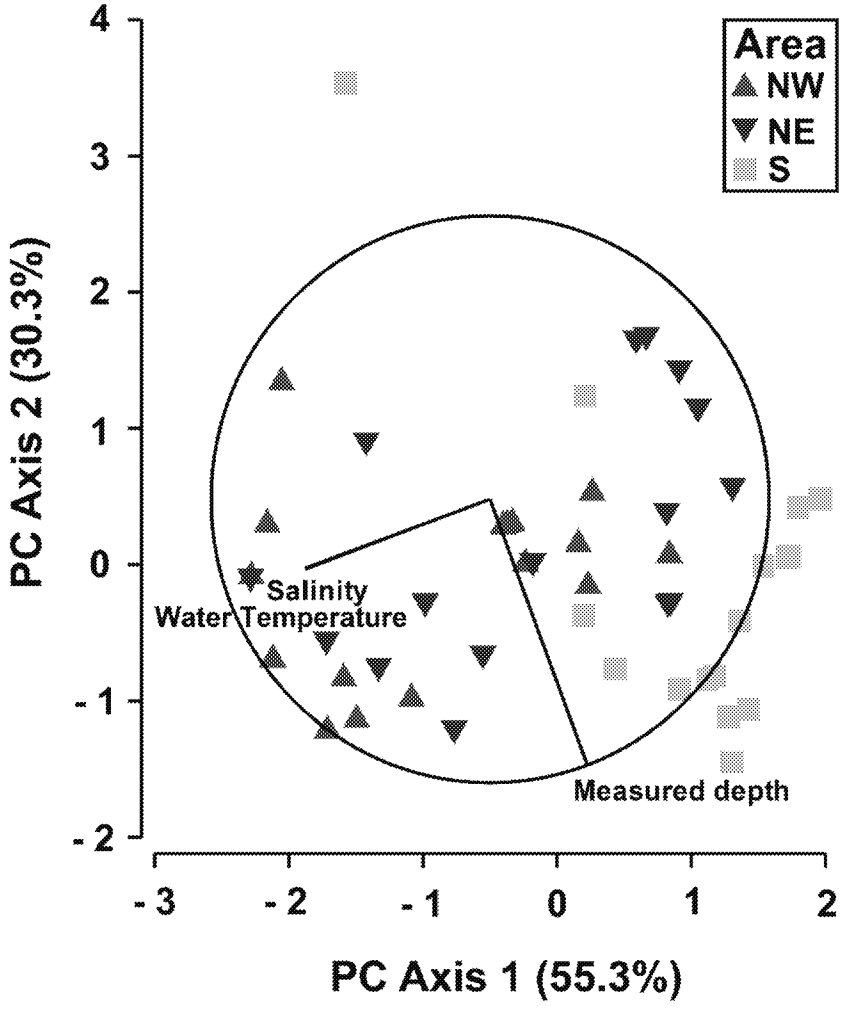

Figure 23. PCA plot of environmental variables (i.e., salinity, measured depth, and water temperature) in the Bahia Grande at 48 macroinvertebrate sampling sites during two sampling events. Black lines indicate the direction in which the associated variable increases.

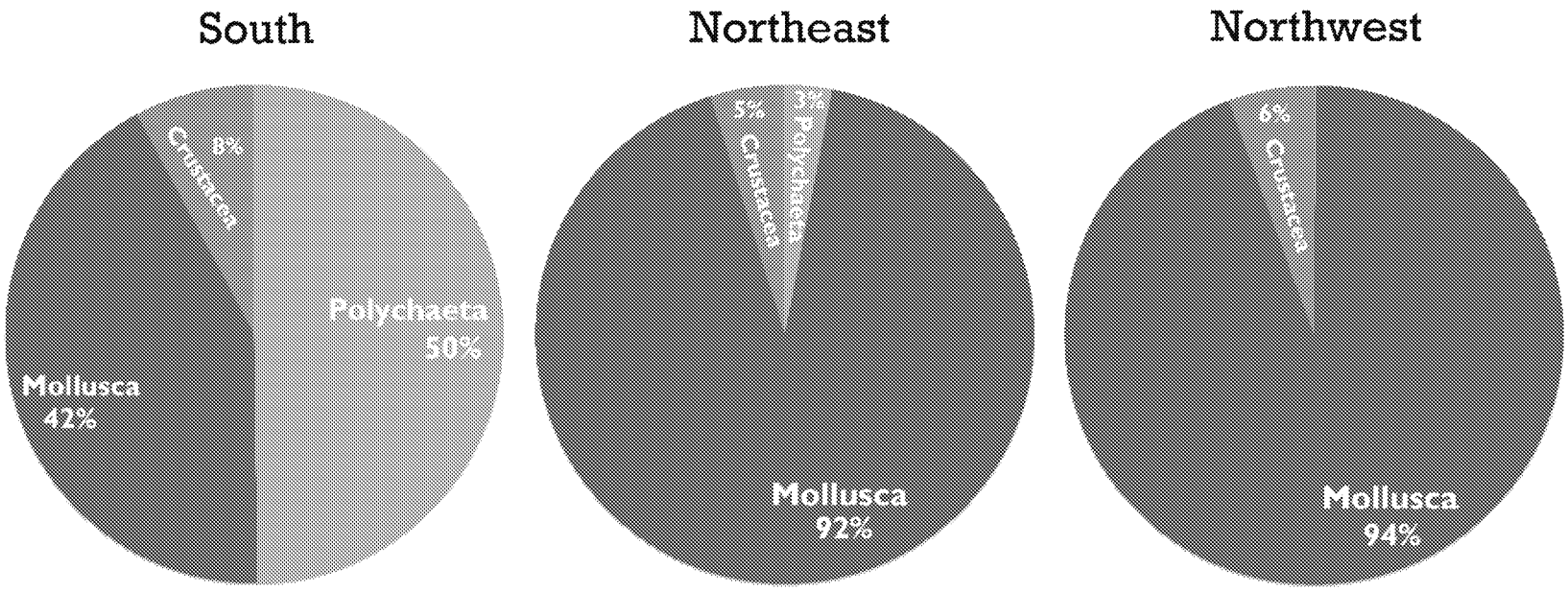

Figure 24. Pie graphs showing the composition of benthic macroinvertebrate communities in three areas of the Bahia Grande (i.e., BG-S, BG-NE, BG-NW). Blue areas represent Mollusca, while green areas represent Crustacea and orange areas represent Polychaeta.

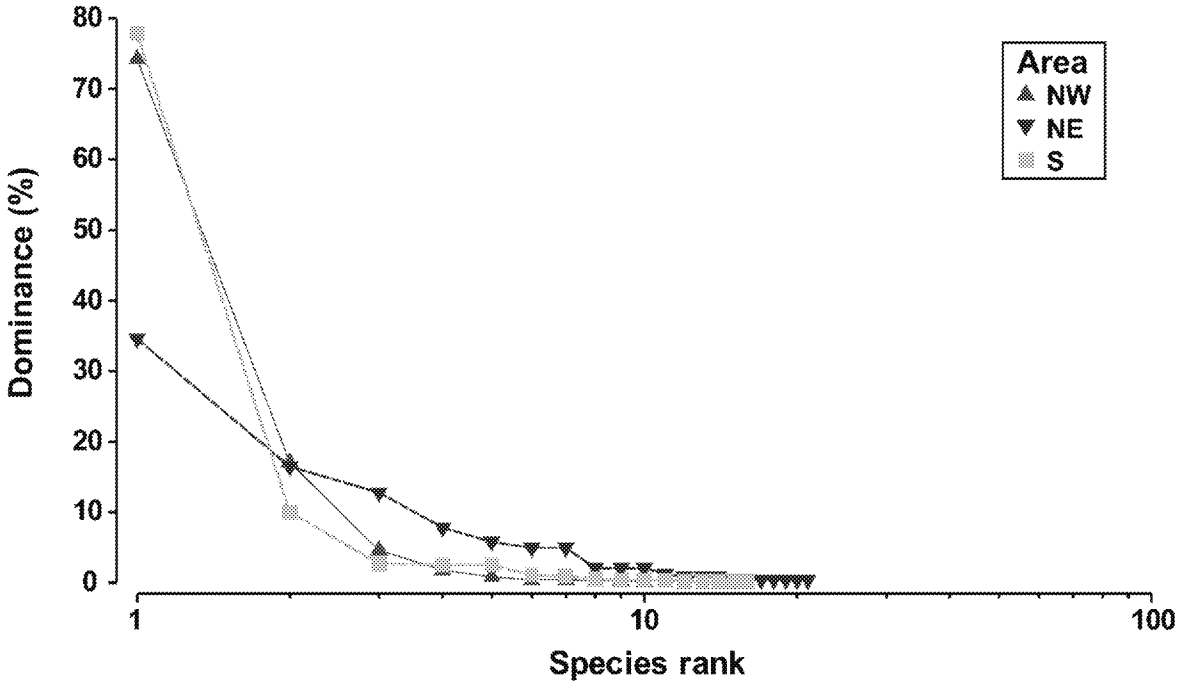

Figure 25. Dominance curve depicting the percentage of the macroinvertebrate community dominated by individual species in each area (i.e., BG-S, BG-NE, and BG-NW). Samples were collected at 48 individual sites in the Bahia Grande.

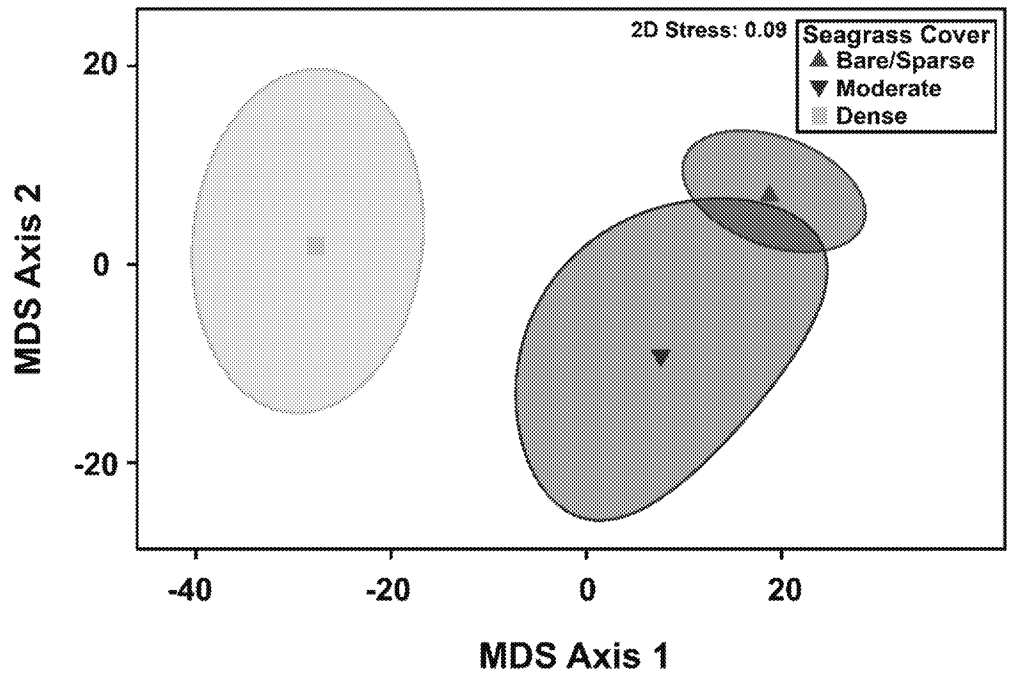

Figure 26. mMDS based on 100 bootstrap averages of macroinvertebrate species abundances in the Bahia Grande at 48 sampling sites grouped by seagrass coverage category (i.e., dense, moderate, and bare/sparse).

CHAPTER IV

DISCUSSION

Salinity and Seagrass Distributions

Sampling to determine salinity trends throughout the re-flooded Bahia Grande revealed differences in salinity among southern and northern areas. The southern area of the basin nearest the inlet channel has the lowest salinities, likely because it is receiving the majority of the tidal water flow into the basin. Salinities are higher in northern areas of the basin, with the northwestern area having the highest salinities. The differences in salinity between northeast and northwest areas of the Bahia Grande are likely due to the patterns of water movement through the railroad trestle that separates the basin into southern and northern halves. There are currently two openings (i.e., cuts) in the railroad trestle that allow boats to move throughout the basin, one of which is on the easternmost side of the trestle, while the other is on the westernmost side of the trestle. The salinity distribution determined in this study indicates that more water is moving through the opening on the northeastern side of the trestle, leading to lower salinities in the northeastern area. More research is needed to fully understand the current movement of water throughout the basin to better inform future restoration actions.

The seagrass distribution map developed as part of this study revealed differences in *H. wrightii* distribution throughout the Bahia Grande. The majority of the southern area of the basin was densely covered with seagrass. The northeastern area was densely covered in areas nearest the opening in the railroad trestle but decreased to moderate and bare/sparse coverage

farther away from that opening. Aside from some areas with moderate coverage near the trestle opening, northwestern areas were almost entirely characterized by little to no seagrass. *H. wrightii* is known to grow at salinities in excess of 60 but dies after 28 days at salinities in excess of 70 (McMahan 1968, McMillan & Moseley 1967). When comparing the salinity and seagrass distribution maps, it appears that *H. wrightii* coverage shifts from moderate to bare/sparse around salinities of 56. It is possible that salinities in this area sometimes reach higher salinities than those measured in this study (e.g., due to an extended lack of rainfall), preventing the long-term establishment of *H. wrightii* beds. In addition, the dense areas near the northeastern trestle opening support the idea that more water is moving through this opening than the northwestern opening, lowering salinities enough for the growth of dense seagrass beds in northeastern areas.

Trace Gases

The results of the sampling methods that were employed to measure trace gas fluxes in Bahia Grande did not support the hypotheses that that fluxes of CO_2 and CH_4 would decrease as salinity increases and increase as seagrass coverage increases. Salinity and seagrass coverage were not selected among the best predictors of trace gas fluxes, and there was no trend based on area or geographic position. These results were unexpected, as both salinity and seagrass coverage have been shown to affect the rate of CO_2 and CH_4 flux in coastal estuaries (Amouroux et al. 2002, Angelis & Lilley 1987, Barber & Carlson 1993, Bartlett et al. 1987, Bouillon et al. 2007, Magenheimer et al. 1996, Purvaja & Ramesh 2001, Upstill-Goddard et al. 2000).

In estuaries ranging from 0 to 35, CH_4 and CO_2 emissions typically decrease with increasing salinity due to the inhibitory effects of high salinities on methanogens and the lack of freshwater input that promotes carbon sequestration (Amouroux et al. 2002, Angelis & Lilley

1987, Bartlett et al. 1987, Craft 2007, Huang et al. 2015, Nyman & DeLaune 1991, Purvaja & Ramesh 2001, Smith et al. 1983, Upstill-Goddard et al. 2000). However, the relationship between CO_2 and CH_4 and salinity in hypersaline estuaries is less well understood due to an overall lack of data. The results of this study suggest that CO_2 and CH_4 fluxes do not decrease any further as salinities increase beyond 35, indicating that hypersalinities (i.e., above 70) do not inhibit methanogenesis and carbon sequestration more than moderate salinities (i.e., ~35).

It was also expected that there would be a relationship between dissolved sulfate concentration and trace gas fluxes in the Bahia Grande. Sulfate, an anion found in natural seawater, inhibits methanogenesis and acts as the primary electron acceptor during respiration, preventing the decomposition of organic matter and subsequent release of CO_2 (Angelis and Lilley 1987, Howarth 1987). In addition, the distribution of sulfate throughout the Bahia Grande was the lowest at the southernmost site and gradually increased in a northern direction. It was expected that sulfate concentrations would be higher in the southern Bahia Grande due to increased tidal flow and exchange. Bartlett et al. (1987) showed that the amount and activity of sulfate reducing bacteria acts as a primary control of not only the amount of sulfate present, but also the subsequent efflux of trace gases. Thus, one possible explanation for the low sulfate concentrations in the southern area of the basin is that the southern areas have more sulfate-reducing bacteria than northern areas and are thus losing sulfate more rapidly through sulfate reduction. In contrast, it is also possible that reduced sulfur compounds are being oxidized at a higher rate in northern areas than in southern areas, leading to higher sulfate concentrations in the northern Bahia Grande.

In addition to the effects of salinity and sulfate on trace gas fluxes, seagrasses are known to provide effectual pathways for the diffusion of both CO_2 and CH_4 between the sediment and

the atmosphere (Bouillon et al. 2007, Purvaja & Ramesh 2001). Thus, the lack of a relationship between seagrass coverage and trace gas fluxes observed in this study is not well understood. It is possible that the high salinity values observed throughout the Bahia Grande have a stronger effect on trace gas fluxes than seagrasses, leading to low flux values throughout the basin regardless of differences in seagrass coverage. Another possible explanation lies in the sampling technique and equipment used in this study. The Los Gatos Dissolved Gas Extraction Unit (DGEU) that was utilized in this experiment has not been used in any other published studies, so it is possible that there were underlying problems with the equipment or user error occurred. More experimental and field test data is needed to fully understand the relationship between user-selected settings (e.g., water flow rate, sweep gas flow rate), the extraction rate of the DGEU, and environmental variables (e.g., water temperature, salinity).

The two variables selected as the best predictors of CO_2 and CH_4 fluxes in the Bahia Grande were water temperature and organic carbon content of the sediment. The relationship between water temperature and the solubility of both CO_2 and CH_4 is well known, with both decreasing as water temperature increases. In addition, in areas with increased carbon accumulation, CO_2 and CH_4 are being removed from the atmosphere to be stored in the sediment. Because of the well-known relationships between trace gas fluxes and both sediment organic carbon and water temperature, it is not surprising that these variables were selected as predicters of CO_2 and CH_4 efflux in the Bahia Grande.

Based on the trace gas flux sampling methods employed in this study, it appears as though trace gas fluxes are not good indicators of rehabilitation in the Bahia Grande. However, it is possible that other trace gas sampling methods would show different results. Future trace gas studies in the Bahia Grande should focus on employing sampling methods that allow for the

measurement of trace gases over longer periods of time and with various equipment in order to better understand the relationship between the salinity gradient, sulfate distribution, and fluxes of CO_2 and CH_4 in the Bahia Grande. A better understanding of the relationship among these variables is needed before attempting to utilize trace gases as an indicator of rehabilitation in the Bahia Grande.

There was not a significant difference in sediment organic carbon and nitrogen content based on location within the basin. The most important predictors of organic content were water temperature and seagrass coverage. It is not surprising that the organic carbon and nitrogen content of the sediment was higher in areas with seagrasses, as leaf litter and belowground biomass are major contributors to the storage of these compounds in the sediment. Similarities in percent organic carbon and nitrogen content of the sediment between areas of dense and moderate seagrass coverage suggests that the presence of seagrass, and not the density, is currently the most important factor controlling the accumulation of organic carbon and nitrogen in the Bahia Grande. The average percent organic carbon content of sediment in bare/sparse, moderate, dense seagrass beds were 2.0, 3.1, 3.4%, respectively, all of which are above the global median of 1.8% organic carbon (Armitage and Fourqurean 2015). Lower levels of organic nitrogen were observed in bare/sparse than in moderate and dense seagrass areas. Low levels of organic nitrogen in coastal sediments are known to limit the establishment of seagrasses (Duarte & Sand-Jensen 1996). Thus, the low levels of nitrogen that exist in bare/sparse areas of the basin could potentially limit the establishment of *H. wrightii* in these areas in the future. The result of the sediment percent organic carbon and nitrogen determinations in this study show that the Bahia Grande has the potential to store large amounts of organic carbon and nitrogen. If further rehabilitation efforts are able to effectively lower salinities in northern areas of the basin,

seagrasses may be able to colonize these areas and increase the carbon and nitrogen storage capacity of the Bahia Grande.

Fish Community Structure

The results of the bag seine and gill net methods that were utilized to assess fish community composition throughout the re-flooded Bahia Grande supported the hypothesis that fish species richness and diversity would decrease as salinity increases. Significant differences between fish communities in BG-S (i.e., lowest salinities) and both BG-NE (i.e., mid salinities) and BG-NW (i.e., highest salinities) were observed. In addition, fish communities in BG-S had higher species richness and diversity than both BG-NE and BG-NW. Depth and salinity were the two most important determining factors of fish community structure in the Bahia Grande. Southern areas of the basin are deeper and less saline, while the northern areas are shallower and more saline. These differences in depth and salinity between areas of the basin are what drove changes in fish community structure in various ways.

While *C. variegatus* dominated fish communities in all three areas of the Bahia Grande, the northern areas were more heavily dominated by this species. Several species, including *P. cromis* and *Lagodon rhomboides*, contributed more to the fish community in BG-S than in the northern areas, lessening the dominance of *C. variegatus* in BG-S. Physiological (e.g., osmotic regulation) and behavioral (e.g., burrowing) adaptations allow *C. variegatus* to survive in environments with salinities ranging from 0 to greater than 140, while many other fish cannot (Bennett & Beitinger 1997, Haney 1999, Nordiie 1985). The absence of competition and predation for *C. variegatus* in extreme environments like the northern areas of the Bahia Grande leads to a community that is highly dominated by one species and low in species richness and diversity. In environments with lower salinities and temperatures (i.e., southern area of the

Bahia Grande), more species are able to survive and compete, leading to a community with lower dominance by *C. variegatus* and higher overall species richness and diversity. The lack of water circulation in and to the northern areas of the Bahia Grande leading to higher salinities, coupled with the lower depths and higher temperatures in northern areas, likely drive the differences in communities between the reference site (i.e., BG-S) and disturbed sites (i.e., BG-S and BG-NW).

The results of sampling efforts also supported the hypothesis that fish species diversity would increase as seagrass coverage increases. Fish communities differed between areas of dense, moderate, and bare/sparse seagrass coverage. Communities within dense seagrass areas were represented most heavily by *P. cromis* and *A. felis*, while both moderate and bare/sparse areas were represented almost entirely by *C. variegatus*. *P. cromis* has been shown to forage primarily in seagrass beds and oyster reefs, while *A. felis* is known to use seagrass beds as reproduction and nursery habitat, explaining the presence of both of these species in areas of dense seagrass coverage (Cave 1978, Dugas 1986, Villéger 2010). Differences in communities between moderate and bare/sparse areas in the Bahia Grande can be attributed to the higher level of dominance by *C. variegatus* in bare/sparse areas. *C. variegatus* has been shown to have high densities in areas with sandy bottoms covered in algae or mangrove litter, while there is not a consistent trend in density related to seagrass bed type (Ellis & Bell 2004, Sheridan 2004). This species also feeds on algae and detritus when they are small (<30 mm) and on crustaceans when they are larger, both of which are abundant in northern areas of the Bahia Grande where salinities are high and seagrass coverage is low (Harrington & Harrigonton 1972, Pfeiffer & Wiegert 1981). Species diversity was higher in areas with dense and moderate seagrass coverage than in bare/sparse areas, likely due to the use of seagrass beds by fishes as permanent habitat,

feeding areas, and refuge from predation (Gray et al. 1996, Jackson et al. 2001). In addition to the effect of seagrass itself, lower salinities in areas with higher seagrass coverage may also promote higher species diversity. The low species richness in dense seagrass areas was likely due to the fewer number of samples within that group rather than a lack of species in these areas.

The differences in fish community structure along salinity and seagrass gradients observed in this study are consistent with other studies that show a decrease in fish richness and diversity with increasing salinity (i.e., in hypersaline estuaries) and decreasing seagrass coverage (Akin et al. 2003, Arrivillaga & Baltz 1999, Barletta et al. 2005, Connolly 1994, Gray et al. 1996, Maes et al. 1998, Martino & Able 2003, Rakocinski et al. 1992, Sosa-Lopez et al. 2007, Vega-Candejas & Hernandez de Santillana 2004). Results from this study are also consistent with those of Cornejo (2009), which showed that fish communities in the Bahia Grande were heavily dominated by *C. variegatus*. Cornejo (2009) also found that the south-to-north salinity gradient was a major determinant of fish community structure throughout the basin, leading to higher species richness and diversity in southern regions of the basin. The similarities between the findings of Cornejo (2009) and this study further support the idea that biotic assemblages in Bahia Grande will likely not change significantly until further restoration actions are complete.

Macroinvertebrate Community Structure

The results of the core sampling and processing methods that were utilized to assess benthic macroinvertebrate community composition throughout the re-flooded Bahia Grande supported the hypothesis that benthic macroinvertebrate richness and diversity would decrease as salinity increases. Significant differences between macroinvertebrate communities in BG-S (i.e., lowest salinities) and BG-NW (i.e., highest salinities) were observed, and communities in BG-S had higher species richness and diversity than both BG-NE and BG-NW. Salinity was the single

most important determining factor of benthic macroinvertebrate community structure in the Bahia Grande. As the geographical position of samples changed in a northwestern fashion, salinities increased and the community of benthic macroinvertebrates changed significantly. The communities of macroinvertebrates in the southern and northern areas differed in several ways.

Polychaetes are typically known to be more resistant to disturbances (e.g., pollution, eutrophication) than crustaceans and mollusks (Dauer 1984, Wildsmith et al. 2010); however, the major perturbation in the Bahia Grande is hypersalinity. Polychaete species richness and diversity have been shown to decrease significantly in response to hypersaline conditions in estuaries, while more resilient bivalves become more dominant (Joydas et al. 2015, Lamptey & Armah 2008). In the Bahia Grande, polychaete worms comprised the largest percentage of macroinvertebrates in the less saline southern area, while mollusks dominated in the more saline northern areas. In addition, the mollusks found in the south were not the same mollusks that dominated in the north. Cerithiidae was the most common mollusk family found in BG-S, while *A. auberiana* and *M. lateralis* dominated BG-NE and BG-NW. Both *A. auberiana* and *M. lateralis* have been shown to tolerate salinities up to 65, with *M. lateralis* able to survive in salinities in excess of 80 (Montagna et al. 1993, Whitelaw DM 2001). In addition, *M. lateralis* is known as a hardy opportunist that is able to colonize rapidly after various disturbances, explaining its widespread abundance in northern areas of the Bahia Grande (Flint & Younk 1983, Flint et al. 1981). While polychaetes comprised 50% of all macroinvertebrates in BG-S, they comprised 3% and 0% in the northeastern and northwestern areas, respectively. Although studies showing the tolerance of polychaete family Capitellidae to hypersaline conditions are generally lacking, Owen & Forbes (1997) showed that capitellids dominated in areas with salinities between 36 and 38 and decreased as salinities fell above or below that range. The lack

of polychaetes and dominance of few molluskan species in the northern areas, specifically in BG-NW, led to the observed differences in species richness, diversity, and community composition.

The differences in macroinvertebrate communities between southern and northern regions, as well as the lack of difference between BG-NW and BG-NE, can largely be attributed to the salinity distribution throughout the Bahia Grande. The lack of water circulation in and to the northern areas of the Bahia Grande causes salinities to increase, leading to changes in macroinvertebrate communities that are heavily dominated by few molluskan species/families and have lower species richness and diversity than the reference site (i.e., BG-S). Although differences in salinities between the two northern regions exist, these differences are evidently not large enough to cause major changes in macroinvertebrate communities.

The results of sampling efforts also supported the hypothesis that macroinvertebrate species diversity would increase as seagrass coverage increases. Macroinvertebrate communities differed between areas of dense, moderate, and bare/sparse seagrass coverage. Communities within dense seagrass areas were represented most heavily by polychaete family Capitellidae, while both moderate and bare/sparse areas were represented almost entirely by molluskan species *A. auberiana* and *M. lateralis*. Differences in communities between moderate and bare/sparse areas can be attributed to the higher level of dominance by *A. auberiana* in moderate areas and *M. lateralis* in bare/sparse areas. While polychaete abundance has been shown to be sensitive to a reduction in seagrass biomass, more opportunistic species like *M. lateralis* are able to fill open niches in the areas with less seagrass that more sensitive polychaete species cannot (Gambi et al. 1998). Benthic macroinvertebrate species richness and diversity in the Bahia Grande was highest in areas with dense seagrass coverage, followed by moderate and bare/sparse

areas, likely due to the protection from predators that seagrass beds provide. In addition to the effect of seagrass itself, lower salinities in areas with higher seagrass coverage may also promote higher species diversity.

Overall, the differences in macroinvertebrate communities based on salinity and seagrass gradients in the Bahia Grande are consistent with the results of various studies that show a decrease in macroinvertebrate richness and abundance with an increase in salinity (i.e., in hypersaline estuaries) and decrease in seagrass coverage (Arrivillaga & Baltz 1999, Attrill et al. 2000, Brucet et al. 2012, Heck & Wetstone 1977, Houte-Howes et al. 2004, Mannino & Montagna 1997, Mills & Berkenbusch 2009, Peterson 1982, Velasco et al. (2002), Velasco et al. 2006, Verschuren et al. 2000, Waterkeyn et al. 2008). The results of this study are also consistent with the results of Tamez (2014). Although Tamez (2014) only collected polychaete data, the overall trend that species richness diversity in the Bahia Grande is low compared to reference sites was similar to the trends observed in this study, further supporting the idea that major changes in biotic communities in the Bahia Grande are unlikely prior to further rehabilitation efforts.

CHAPTER V

CONCLUSIONS & RESTORATION SUGGESTIONS

The present study revealed that the southern area of the Bahia Grande is characterized by lower salinities and higher seagrass coverage than northern areas, leading to higher sediment carbon and nitrogen content and higher macroinvertebrate and fish species richness and diversity. The differences in water parameters, carbon and nitrogen content, and faunal communities throughout the basin indicates a lower level of rehabilitation in northern, particularly northwestern, areas of the Bahia Grande compared to the southern reference area. Salinity and seagrass distribution maps suggest that the northeastern area of the basin is receiving more water flow than the northwestern area, although neither are receiving enough tidal exchange to maintain low enough salinities to support widespread seagrass coverage and healthy faunal communities. The most likely factors leading to prolonged hypersalinity in northern areas of the basin are the size of the pilot channel (4.5 m wide) and the historic railroad trestle dividing the basin into southern and northern halves. These impediments to water flow limit the faunal communities in northern areas primarily to species able to tolerate extreme hypersalinities (e.g., *C. variegatus*, *M. lateralis*, *A. auberiana*).

Until tidal exchange throughout the basin increases and salinities in northern areas decrease, the value of the Bahia Grande as a nursery habitat for commercially important juvenile fishes (e.g., red drum, black drum, spotted seatrout) will be greatly diminished. Although adults

of the aforementioned species were found in northern areas of the Bahia Grande and are thus able to withstand the higher salinities, larvae, eggs and juveniles of the same species are more sensitive to high salinities and are thus unlikely to survive (Banks et al. 1991, Gray et al. 1991). Managing salinities in the Bahia Grande is crucial to its rehabilitation and increasing circulation throughout the basin should be of primary focus when considering future rehabilitation efforts.

Based on the findings of this study, further interventions are recommended in order to fully restore the Bahia Grande to a functioning estuary. Although already scheduled, widening the pilot channel into the Bahia Grande will allow for more water exchange per tidal cycle, potentially lowering salinities throughout the basin. The effectiveness of the widened channel depends on the width of the channel, the flow rate it can sustain, and the movement of tidal waters throughout the basin. Thus, in order for the widened channel to function optimally, barriers to water flow within the basin (i.e., railroad trestle, cattle fences) should be minimized. If complete removal of barriers is not feasible, creating more openings (i.e., cuts) within the barriers is recommended to maximize water flow between southern and northern areas. Lowering salinities in northern areas of the basin through further restoration actions would not only promote higher faunal richness and diversity on its own, but also allow seagrasses to establish in new areas. These newly established seagrass beds would not only provide the habitat and protection needed to support various faunal species, but also increase the capacity of the basin to store carbon and nitrogen in sediments.

This study not only provides insight into the restoration status of the Bahia Grande estuary, but also provides valuable baseline data that can be used for comparison with conditions after the widening of the inlet channel is complete. In addition to follow-up assessments to determine changes in salinities, seagrasses, and faunal communities due to channel widening,

studies to determine flow rates and tidal exchange in various areas of the Bahia Grande would provide valuable information about areas of the basin that may require further intervention. Although the Bahia Grande is not yet entirely recovered, restoring the system to a fully functioning estuarine ecosystem is possible through properly informed interventions and management practices.

REFERENCES

Akin S, Winemiller KO, Gelwick FP. 2003. Seasonal and spatial variations in fish and macrocrustacean assemblage structure in Mad Island Marsh estuary, Texas. Estuarine, Coastal and Shelf Science. 57:269-282.

Amouroux D, Roberts G, Rapsomanikis S, Andreae MO. 2002. Biogenic gas (CH_4, N_2O, DMS) emission to the atmosphere from near-shore and shelf waters of the north-western Black Sea. Estuarine, Coastal and Shelf Science. 54:575-587.

Angelis MA, Lilley MD. 1987. Methane in surface waters of Oregon estuaries and rivers. Limnol. Oceanogr. 32:716-722.

Armitage AR, Fourqurean JW. 2015. Carbon storage in seagrass soils: long-term nutrient history exceeds the effects of near-term nutrient enrichment. Biogeosciences. 13:313-321.

Arrivillaga A, Baltz DM. 1999. Comparison of fishes and macroinvertebrates on seagrass and bare-sand sites on Guatemala's Atlantic coast. Bulletin of Marine Science. 65(2):301-319.

Attrill MJ, Strong JA, Rowden AA. 2000. Are macroinvertebrate communities influenced by seagrass structural complexity? Ecography. 23:114-121.

Bange HW, Bartell UH, Rapsomanikis S, Andreae MO. 1994. Methane in the Baltic and North Seas and a reassessment of the marine emissions of methane. Global Biogeochemical Cycles. 4:465-480.

Banks MA, Holt GJ, Wakeman JM. 1991. Age-linked changes in salinity tolerance of larval spotted seatrout (*Cynoscion nebulosus*, Cuvier). Fish Biology. 39(4):505-514.

Barber TR, Carlson PR. 1993. Effects of seagrass die-off on benthic fluxes and porewater concentrations of ΣC02, ΣH2S, and CH4 in Florida Bay sediments. Biogeochemistry of Global Change: Radiatively Active Trace Gases. 530-550.

Barletta M, Barletta-Bergan A, Saint-Paul U, Hubold G. 2005. The role of salinity in structure the fish assemblages in a tropical estuary. Journal of Fish Biology. 66:45-72.

Bartlett KB, Bartlett DS, Harriss RC, Sebacher DI. 1987. Methane emissions along a salt marsh salinity gradient. Biogeochemistry. 4:183-202.

Bennett WA, Beitinger TL. 1997. Temperature tolerance of the sheepshead minnow, *Cyprinodon variegatus*. American Society of Ichthyologists and Herpetologists. 1:77-87.

Bouillon S, Dehairs F, Velimirov B, Abril G, Borges AV. 2007. Dynamics of organic and inorganic carbon across contiguous mangrove and seagrass systems (Gazi Bay, Kenya). Journal of Geophysical Research. 112:1-14.

Brucet S, Boix D, Nathansen LW, Quintana XD, Jansen E, Balayla D, Meerhoff M, Jeppesen E. 2012. Effects of temperature, salinity and fish structuring the macroinvertebrate community in shallow lakes: implications for effects of climate change. PLoS ONE. 7(2):1-11.

Cave N. 1978. Predator-prey relationships involving the American oyster, *Crassostreavirginica*, and the black drum, *Pogonias cromis*, in Mississippi Sound. Southeastern Louisiana University: A Thesis.

Connolly RM. 1994. A comparison of fish assemblages from seagrass and unvegetated areas of a southern Australian estuary. Aust. J. Mar. Freshwater Res. 45:1033-1044.

Cornejo EM. 2009. Fish assemblage dynamics in the re-flooded Bahia Grande. The University of Texas Rio Grande Valley: A Thesis.

Craft C. 2007. Freshwater input structures soil properties, vertical accretion, and nutrient accumulation of Georgia and U.S. tidal marshes. Limnol. Oceanogr. 52(3):1220-1230.

Dauer DM. 1984. High resilience to disturbance of an estuarine polychaete community. Bulletin of Marine Science. 34(1):170-174.

Duarte CM, Sand-Jensen K. 1996. Nutrient constraints on establishment from seed and on vegetative expansion of the Mediterranean seagrass *Cymodocea nodosa.* Aquatic Botany. 54(4):279-286.

Dugas, CN. 1986. Food habits of black drum, *Pogonias cromis*, in southeast Louisiana with emphasis on their predation of the American oyster, Crassostrea virginica. Louisiana Department of Wildlife and Fisheries.

Ellis WL, Bell SS. 2004. Conditional use of mangrove habitats by fishes: depth as a cue to avoid predators. Estuaries. 27(6):966-976.

Flint RW, Kalke RD, Rabalais SC. 1981. Quantification of extensive freshwater input to estuarine benthos. Report to the Texas Water Development Board. 55pp.

Flint RW, Younk JA. 1983. Estuarine benthos: long-term variations. Estuaries. 6:126-141.

Fourqurean JW, Kendrick GA, Collins LS, Chambers RM, Vanderklift MA. 2012. Carbon, nitrogen and phosphorus storage in subtropical seagrass meadows: examples from Florida Bay and Shark Bay. Marine and Freshwater Research. 63:967-983.

Frankignoulle M, Abril G, Borges A, Bourge I, Canon C, Delille B, Libert E, Theate JM. 1998. Carbon dioxide emission from European estuaries. Science. 282:434-436.

Gambi MC, Conti G, Bremec CS. 1998. Polychaete distribution, diversity and seasonality related to seagrass cover in shallow soft bottoms of the Tyrrhenian Sea (Italy). Scientia Marina. 62(1-2):1-17.

Gray CA, McElligott DJ, Chick RC. 1996. Differences in assemblages of fishes associated with shallow seagrass and bare sand. Mar. Freshwater Res. 47:723-735.

Gray JD, King TL, Colura RL. 1991. Effect of temperature and hypersalinity on hatching success of spotted seatrout eggs. The Progressive Fish Culturalist. 53(2):81-84.

Haney DC. 1999. Osmoregulation in the sheepshead minnow, Cyprinodon variegatus: influence of a fluctuating salinity regime. Estuaries. 22(4):1071-1077.

Harrington RW, Harrington ES. 1972. Food of female marsh killifish, *Fundulus confluentus* Goode and Bean, in Florida. The University of Notre Dame. 87(2):492-502.

Heck KL, Wetstone GS. 1977. Habitat complexity and invertebrate species richness and abundance in tropical seagrass meadows. Journal of Biogeography. 4:135-142.

Hicks DW, DeYoe H, Whelan T, Benavides J, Shands MJ, Heise E. 2010. Bahia Grande restoration monitoring final report. United States Environmental Protection Agency.

Houte-Howes KSS, Turner SJ, Pilditch CA. 2004. Spatial differences in macroinvertebrate communities in intertidal seagrass habitats and unvegetated sediment in three New Zealand estuaries. Estuaries. 27(6):945-957.

Howard J, Hoyt S, Isensee K, Telszewski M, Pidgeon E. 2014. Coastal blue carbon: Methods for assessing carbon stocks and emissions factors in mangroves, tidal salt marshes, and seagrass meadows. The Blue Carbon Initiative. 1-184.

Howarth RW. 1984. The ecological significance of sulfur in the energy dynamics of salt marsh and coastal marine sediments. Biogeochemistry. 1:5-27.

Huang WJ, Cai WJ, Wang Y, Lohrenz SE, Murrell MC. 2015. The carbon dioxide system on the Mississippi River-dominated continental shelf in the northern Gulf of Mexico: 1. Distribution and air-sea CO_2 flux. Journal of Geophysical Research: Oceans. 120:1429-1445.

Jackson EL, Rowden AA, Attrill MJ, Bossey SJ, Jones MB. 2001. The importance of seagrass beds as a habitat for fishery species. Oceanography and Marine Biology: An Annual Review. 39:269-303.

Joydas TV, Qurban MA, Manikandan KP, Ashraf TTM, Ali SM, Abdulkader K, Qasem A, Krishnakumar PK. 20115. Status of microbenthic communities in the hypersaline waters of the Gulf of Salwa, Arabian Gulf. Journal of Sea Research. 99:34-36.

Kefford BJ. 2000. The effect of saline water disposal: implications for monitoring programs and management. Environmental Monitoring and Assessment. 63:313-327.

Lamptey E, Armah AK. 2008. Factors affecting microbenthic fauna in a tropical hypersaline coastal lagoon in Ghana, West Africa. Estuaries and Coasts. 31(5):1006-1019.

Lichlyter SA. 2006. An applied paleoecology case study: Bahia Grande, Texas prior to construction of the Brownsville Ship Channel. Texas A&M University: A Thesis.

Maes J, Damme PA, Taillieu A, Ollevier F. 1998. Fish communities along an oxygen-poor salinity gradient (Zeeschelde Estuary, Belgium). Journal of Fish Biology. 52:534-546.

Magenheimer JF, Moore TR, Chmura GL, Daoust RJ. 1996. Methane and carbon dioxide flux from a macrotidal salt marsh, Bay of Fundy, New Brunswick. Estuaries. 19(1):139-145.

Mannino A, Montagna PA. 1997. Small-scale spatial variation of macrobenthic community structure. Estuaries. 20(1):159-173.

Marba N, Arias-Ortiz A, Masque P, Kendrick GA, Mazarrasa I, Bastyan GR, Garcia-Orellana J, Duarte CM. Impact of seagrass loss and subsequent revegetation on carbon sequestration and stocks. Journal of Ecology. 103:296-302.

Marquez MA, Fierro-Cabo A and Cintra-Buenrostro CE. 2017. Can ecosystem functional recovery be traced to decomposition and nitrogen dynamics in estuaries of the Lower Laguna Madre, Texas? Restoration Ecology. 24(4):618-628.

Martinez C. 2015. *Balanus eberneus* (Crustacea: Cirripedia) as a potential indicator of estuarine system recovery in South Texas: a study of recruitment, growth, and stable isotopes. The University of Texas Rio Grande Valley: A Thesis.

Martino EJ, Able KW. 2003. Fish assemblages across the marine to low salinity transition zone of a temperature estuary. Estuarine, Coastal and Shelf Science. 56:969-987.

Mcleod E, Chmura GL, Bouillon S, Salm R, Bjork M, Duarte CM, Lovelock CE, Schlesinger WH, Silliman BR. 2011. Front Ecol. Environ. 9(10):552-560.

McMahan CA. 1968. Biomass and salinity tolerance of shoalgrass and manateegrass in Lower Laguna Madre, Texas. The Journal of Wildlife Management. 32(3):501-506.

McMillan C, Moseley FN. 1967. Salinity tolerances of five marine spermatophytes of Redfish Bay, Texas. Wiley, Ecological Society of America. 48(3):503-506.

Mills VS, Berkenbusch K. 2009. Seagrass (*Zostera muelleri*) patch size and spatial location influence infaunal macroinvertebrate assemblages. Estuarine, Coastal and Shelf Science. 81:123-129.

NOAA (National Oceanic and Atmospheric Administration), Halpert MS and Bell GD. 1996. Climate Assessment for 1996.

Nyman JA, DeLaune RD. 1991. CO_2 emission and soil Eh responses to different hydrological conditions in fresh, brackish, and saline marsh soils. Limnol. Oceanogr. 36(7):1406-1414.

Orth RJ, Heck KL, van Montfrans J. 1984. Faunal communities in seagrass beds: a review of the influence of plant structure and prey characteristics on predator: prey relationships. Estuaries. 7(4):339-350.

Owen RK, Forbes AT. 1997. Salinity, floods and the infaunal microbenthic community of the St. Lucia estuary, Kwazalu-Natal, South Africa. Southern African Journal of Aquatic Science. 23(1):14-30.

Pfeiffer WJ, Wiegert RG. 1981. Grazers on Spartina and their predators. Ecological Studies. 38:87-112.

Poffenbarger HJ, Needelman BA, Megonigal JP. 2011. Salinity influence on methane emissions from tidal marshes. Wetlands 31:831-842.

Purvaja R, Ramesh R. 2001. Natural and anthropogenic methane emission from coastal wetlands of South India. Environmental Management. 27(4):547-557.

Rakocinski CF, Baltz DM, Fleeger JW. 1992. Correspondence between environmental gradients and the community structure of marsh-edge fishes in a Louisiana estuary. Mar. Ecol. Prog. Ser. 80:135-148.

Russell BD. 2013. Future seagrass beds: can increased productivity lead to increased carbon storage? Mar. Pollut. Bull. Article in Press.

Sheridan P. 2004. Comparison of restored and natural seagrass beds near Corpus Christi, Texas. Estuaries. 27(5): 781-792.

Smith CJ, DeLaune RD, Patrick WH. 1983. Carbon dioxide emissions and carbon accumulation in coastal wetlands. Estuarine, Coastal and Shelf Science. 17:21-29.

Sosa-Lopez A, Mouillor D, Ramos-Miranda J, Flores-Hernandez D, Do Chi T. 2007. Fish species richness decreases with salinity in tropical coastal lagoons. Journal of Biogeography. 34:52-61.

Sun Z, Wang L, Tian H, Jiang H, Mou X, Sun W. 2013. Fluxes of nitrous oxide and methane in different coastal *Suaeda salsa* marshes of the Yellow River estuary, China. Chemosphere. 90:856-865.

Tamez CA. 2014. Gauging wetland restoration status using benthic-based structural and functional metrics. Unpublished.

Telesh IV, Khlebovich VV. 2010. Principal processes within the estuarine salinity gradient: a review. Marine Pollution Bulletin. 61:149-155.

Upstill-Goddard RC, Barnes J, Frost T, Punshon S, Owens NJP. 2000. Methane in the southern North Sea: low-salinity inputs, estuarine removal, and atmospheric flux. Global Biogeochemical Cycles. 14(4):1205-1217.

USFWS (U.S. Fish and Wildlife Service). 2004. Laguna Atascosa National Wildlife Refuge, South Texas Refuge Complex, proposed re-flooding and restoration of Bahia Grande: Final draft (environmental assessment). 47 p.

Van Horn DJ, Okie JG, Buelow HN, Gooseft MN, Barrett JE, Takacs-Vesbach CD. 2014. Soil microbial responses to increased moisture and organic resources along a salinity gradient in a polar desert. Appl. Environ. Microbiol.

Vega-Candejas ME, Hernandez de Santillana M. 2004. Fish community structure and dynamics in a coastal hypersaline lagoon: Rio Lagartos, Yucatan, Mexico. Estuarine, Coastal and Shelf Science. 60:285-299.

Velasco J, Millan A, Hernandez J, Gutierrez C, Abellan P, Sanchez D, Ruiz M. 2004. Response of biotic communities to salinity changes in a Mediterranean hypersaline stream. Saline Systems. 2:12.

Villéger S, Miranda JR, Hernández DF, Mouillot D. 2010. Contrasting changes in taxonomic vs. functional diversity of tropical fish communities after habitat degradation. Ecological Applications. 20(6).

Waterkeyn A, Grillas P, Vanschoenwinkel B, Brendonck L. 2008. Invertebrate community patterns in Mediterranean temporary wetlands along hydroperiod and salinity gradients. Freshwater Biology. 53:1808-1822.

Whitelaw DM. 2001. Assessment of the hydrological impact of conduits on the distribution of biota in an inland saline pond, San Salvador Island, Bahamas. Proceedings of the 10th Symposium on the Geology of the Bahamas and Other Carbonate Regions. 41-53.

Wildsmith MD, Rose TH, Potter IC, Warwick RM, Clarke KR. 2011. Benthic macroinvertebrates as indicators of environmental deterioration in a large microtidal estuary. Marine Pollution Bulletin. 62(3):525-538.

Williams WD. 1999. Salinisation: a major threat to water resources in the arid and semi-arid areas of the world. Lakes & Reservoirs: Research and Management. 4:85-91.

Zeng CS, Wang WQ, Tong C. 2008. Effects of different exogenous electron acceptors and salt import on methane production potential of estuarine marsh soil. Geogr. Res. 27:1321-1330.

APPENDIX A

APPENDIX A

TRACE GAS FLUXES, SULFATE CONCENTRATIONS & SEDIMENT ORGANIC CARBON AND NITROGEN CONTENTS

Site	CO_2 (μ mol/m^2/sec)	CH_4 (μ mol/m^2/sec)	Organic C (%)	Total N (%)	Sulfate (mg/L)
S1	0.088	-0.017	0.96	0.02	2990
S2	-0.272	-0.020	1.42	0.02	3000
S3	-0.050	-0.011	2.24	0.06	3230
S4	0.006	-0.006	2.88	0.12	3160
S5	0.648	0.012	4.05	0.25	3210
S6	0.668	0.007	2.91	0.16	3120
S7	0.692	0.032	4.25	0.24	3430
S8	0.019	-0.015	3.87	0.22	3330
S9	0.543	0.052	4.88	0.38	3480
N1	0.456	0.031	4.18	0.23	3910
N2	0.075	-0.018	6.04	0.43	3850
N3	-0.452	-0.047	1.92	0.05	4240
N4	-0.011	-0.012	1.59	0.07	5690
N5	0.170	-0.008	2.90	0.13	6190
N6	0.065	0.021	1.85	0.03	6470
N7	0.050	-0.002	2.46	0.11	6480
N8	-0.072	0.008	1.92	0.05	6450
N9	-0.026	0.005	2.56	0.09	6250

APPENDIX B

APPENDIX B

FISH SPECIES ABUNDANCES

Species	**BG-S**	**BG-NE**	**BG-NW**	**N**	**%***
Cyprinodon variegatus	1778	763	950	3491	57.92
Pogonias cromis	662	1	64	727	12.06
Lagodon rhomboides	483	1	3	487	8.08
Menidia sp.	235	28	94	357	5.92
Fundulus grandis	182	4	18	204	3.38
Mugil curema	20	0	173	193	3.20
Brevoortia patronus	179	0	0	179	2.97
Mugil cephalus	16	136	8	160	2.65
Fundulus similis	38	27	1	66	1.10
Ariopsis felis	51	6	3	60	1.00
Leiostomus xanthurus	8	11	0	19	0.32
Eucinostomus argenteus	18	0	0	18	0.30
Sciaenops ocellatus	15	3	0	18	0.30
Elops saurus	3	2	8	13	0.22
Cynoscion nebulosus	11	0	0	11	0.18
Strongylura marina	7	0	0	7	0.12
Sphoeroides parvus	5	0	0	5	0.08
Caranx hippos	4	0	0	4	0.07
Eucinostomus melanopterus	3	0	0	3	0.05
Syngnathus scovelli	0	2	0	2	0.03
Archosargus probatocephalus	0	0	2	2	0.03
Centropomus undecimalis	1	0	0	1	0.02
Totals	3719	984	1324	6027	100.00

*: total relative abundance

APPENDIX C

APPENDIX C

MACROINVERTEBRATE SPECIES ABUNDANCES

Species	**BG-S**	**BG-NE**	**BG-NW**	**N**	**%***
Anomalocardia auberiana	31	437	548	1016	65.97
Mulinia lateralis	19	56	124	199	12.92
Capitellidae	84	14	0	98	6.36
Aoridae	12	14	34	60	3.90
Cerithiidae	40	5	13	58	3.77
Amygdalum papyrium	5	15	3	23	1.49
Spionidae	14	2	1	17	1.10
Columbellidae	5	1	6	12	0.78
Nemertea	12	0	0	12	0.78
Corophiidae	1	3	3	7	0.45
Idoteidae	1	6	0	7	0.45
Orbiniidae	5	0	0	5	0.32
Collembola	1	1	2	4	0.26
Cumacea	1	1	2	4	0.26
Farfantepenaeus aztecus	2	1	0	3	0.19
Maldanidae	3	0	0	3	0.19
Harpaticidae	0	2	0	2	0.13
Chione elevata	2	0	0	2	0.13
Gammaridae	0	2	0	2	0.13
Polydora	2	0	0	2	0.13
Ampharetidae	1	0	0	1	0.06
Oligochaeta	0	1	0	1	0.06
Callinectes similis	1	0	0	1	0.06
Neritina virginea	1	0	0	1	0.06
Totals	243	561	736	1540	100.00

*: total relative abundance

BIOGRAPHICAL SKETCH

Catherine M. Eckert attended high school at Hyde Park Baptist High School in Austin, Texas from 2007 to 2011, where she earned her high school degree. After graduating high school, Catherine attended Rhodes College in Memphis, Tennessee from 2011 to 2016, where she earned her Bachelor of Science in Biology. Catherine started her work in the biological sciences field in 2017 at Capitol Reef National Park in Utah, where she worked as a biological science technician for AmeriCorps. After working in Utah for seven months, Catherine moved back to Texas and earned her Master of Science in Biology degree at The University of Texas Rio Grande Valley in December 2019. Catherine can be reached by mail at 13322 Shore Vista Dr, Austin, TX 78732 or by email at cateckert22@gmail.com.